Spectral Trends in GC-EI-MS Data Obtained from the SWGDRUG Library and Literature: A Resource for the Identification of Unknown Compounds

William Feeney[a*], Arun S. Moorthy[a], Edward Sisco[a]
[a]National Institute of Standards and Technology, Gaithersburg, MD, USA
*william.feeney@nist.gov

Abstract

Rapid identification of new or emerging psychoactive substances remains a critical challenge in forensic drug chemistry laboratories. Current analytical protocols are well-designed for confirmation of known substances yet struggle when new compounds are encountered. Many laboratories initially attempt to classify new compounds using gas chromatography mass spectrometry (GC-MS) data. Though there is a large body of research focused on analysis of illicit substances with GC-MS, there is little high-level discussion of mass spectral trends for different classes of drugs. This manuscript compiles literature information and performs simple exploratory analyses on evaluated GC-MS data to investigate trends of electron ionization (EI) mass spectra on the most reported illicit substance classes. Additionally, this work offers other important aspects: brief discussions of how each class of drugs is used; descriptions of proposed fragmentation pathways of commonly observed ions in EI-MS data; and summaries of mass spectral trends that can help an analyst classify new illicit compounds.

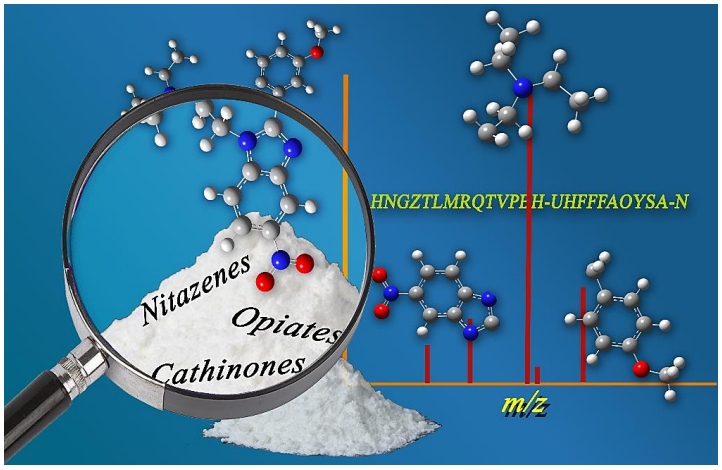

Keywords: Drug trends, novel psychoactive substances (NPS), GC-EI-MS, fragmentation pathways, seized drug

Highlights

- Reviews current literature and compares spectra in SWGDRUG library
- Provides brief description of drug class origin and effects within the body
- Illuminates shared characteristics in molecular and product ion intensities
- Identifies mass spectral trends within common drugs-of-abuse and NPSs

1. Introduction

In recent years, forensic laboratories have reported an influx of new illicit drugs [1–7]. Among the traditional substances reported, new/novel psychoactive substances (NPSs) or emerging synthetic drugs are becoming more prevalent because they (i) produce equivalent psychoactive responses by targeting similar receptors and reaction sites within the body, (ii) elude legal definitions of a controlled substance, and (iii) evade detection due to identification limitations [6–13]. These substances incorporate a variety of classes including, but not limited to – cannabinoids, opioids, stimulants, and benzodiazepines [2,3]. These broad classes are comprised of various subcategories that share psychotropic effects, chemical structures, or legal definitions. For example, the opioids class consists of fentanyl-related compounds (FRC), opiates, utopioids, and the newly emerging nitazenes [10,14,15]. The emergence of these chemically diverse NPSs brings new analytical challenges for current instrumentation practices to identify and classify seized samples.

In traditional seized drug analysis, gas chromatography-electron ionization-mass spectrometry (GC-EI-MS) is one preferred technique for practitioners and is identified by the Scientific Working Group for the Analysis of Seized Drugs (SWGDRUG) as an effective tool for analysis [16–20]. Briefly, in EI, volatile compounds are ionized via the bombardment of highly energetic electrons (70 eV) from a heated filament causing an ejection of an analyte's orbital electrons producing a radical cation [21,22]. This process provides excess energy to the analyte resulting in fragment ions displayed in a mass spectrum which is composed of mass-to-charge (*m/z*) values and abundances as well as natural isotopic abundances [21,22]. Laboratories benefit from a massive, evaluated mass spectral library of reproducible EI-MS fragmentation from which an unknown and known spectra can be compared to postulate a compound's identification. With the introduction of NPSs, however, subtle alterations to the core chemical structure can result in nearly indistinguishable spectra and lead to misclassifications [8,10,23,24]. Alternatively, if emerging compounds are not present in the library, the mass spectrum may not provide a good match to any entry and thus, may lead chemists to attempt to identify spectral trends based on drug classes.

The goal of this work is to condense results of previous studies and to provide guidance into EI mass spectra trends across NPS classes. This paper also reviews literature of the most encountered classes [6] of NPSs and summarizes EI mass spectral trends for these drugs through an analysis of the SWGDRUG Mass Spectral Library [19]. The merged database investigation

performed highlights mass spectral properties and identified the most frequent ions within the classes. Finally, this work can serve as a reference guide for current observations and assist in narrowing potential classifications for unknown spectra.

2. Methods

2.1. Preprocessing to produce class database

To complete class-based analyses, class identifications were obtained from the Cayman Chemical product catalog and appended to the entries within the SWGDRUG GC-MS library (version 3.10) [19] using a custom *R* script described in the *Supplemental Information*. The resulting dataset, referred to as the *merged database*, yielded over 1,500 entries across seven broad classes and fifteen subclasses [6], the distribution of which is shown in **Table 1**. It is important to mention that this process is automated and thus, there are some compounds that are members of multiple classes. For example, N-benzylpiperazine (BZP) and escaline are included in both stimulant and hallucinogen classes.

Table 1: Summary of drug classes in the merged database discussed (*n*=1,544).

Broad Class	Subclass Breakdown
Barbiturates *(n=10)* (**Section 3.1.1.**)	*N/A*
Benzodiazepines *(n=56)* (**Section 3.1.2.)**	*N/A*
Anabolic Steroids *(n=50)* (**Section 3.1.3.**)	*N/A*
Cannabinoids *(n=448)* (**Section 3.1.4.**)	Phytocannabinoids *(n=24)* Synthetic Cannabinoids *(n= 424)*
Opioids *(n=323)* (**Section 3.1.5.**)	Fentanyls *(n=237)* Nitazenes *(n=15)* Opiates *(n=36)* Utopiods *(n=35)*
Stimulants *(n=600)* (**Section 3.1.6.**)	Amphetamines *(n=174)* Arylcyclohexylamines *(n=42)* Cathinones *(n=229)* Phenethylamines *(n=127)* Piperazines *(n=28)*
Hallucinogens *(n=57)* (**Section 3.1.7.**)	Tryptamines (*n=57*)

To capture class similarities, the peaks in the mass spectra were binned into one of five categories depending on their relative intensity/abundance (RA) – *Base Peak* (*m/z* values with a RA of 100 %), *High* (*m/z* values with RAs of 50 % to 99 %), *Medium* (*m/z* values with RAs of 10 % to 50 %), *Low* (*m/z* values with RAs of 5 % to 10 %), and *Ultra-Low* (*m/z* values with RAs of less than 5 %).

2.2. Data analysis

After verification of the merged database, a simple merged database investigation was conducted to measure the occurrence of *m/z* values within each RA category to illuminate potential trends and common fragments shared within each class. The *Ultra-Low* and *Low* RA categories are not discussed comprehensively in this manuscript as they are often not above critical thresholds or limits-of-detection (LOD) in experimental data or, especially for *Ultra-Low* peaks, may be noise. As a starting point, the top 10 reoccurring ions are presented for each category. To provide further insight into the structures of frequently occurring ions, proposed fragmentation pathways found in relevant literature have been included. The *NIST MS Interpreter* tool version 3.4.4 (available at chemdata.nist.gov) was utilized to elucidate structures when minimal literature was found. Additionally, neutral losses were investigated to highlight fragmentation commonalities that are not directly observable in a mass spectrum. Neutral losses were calculated by taking the difference between the molecular ion (or known molecular mass) and the observed fragment ions.

3. Results and Discussion

3.1. Mass spectra trends within each class

The following sections involve discussions and breakdowns of EI-MS trends for the frequently encountered drug classes that have at least 10 compounds present in the merged database [2,6,7]. Each section contains a description of their use, relevancy in casework, common core structure substitutions, common fragmentation pathways, and a table showing top reoccurring ions from the merged database for *Base Peak*, *High*, and *Medium* RA categories. The number of peaks across these bins, as well as the *Low* RA category, and where these *m/z* range peaks are commonly observed is also reported. The top reoccurring neutral losses across these RA categories are also provided. The *Ultra-Low* peaks were not considered in this study due to the potential difficulty in distinguishing from background noise.

For each section, a figure is also provided to summarize important information. Each figure depicts the core structure(s) of the class and, when appropriate, example fragmentation pathways. Three plots are also provided. The first plot provides a representation of the average distribution of peaks in this mass spectrum – plotting the average number of peaks observed for *Low*, *Medium*, and *High + Base Peak* RA categories binned into 40 *m/z* increments across the mass scan range. The second plot is designed to show how feature-rich the mass spectra for the class are by plotting the average number of *Low*, *Medium*, and *High + Base Peaks*. The y-axis of this plot is fixed

across in all figures to allow for class-to-class comparisons. The third plot provides information on the presence, and abundance, of molecular ions. As the purpose of this manuscript is to provide a resource for the classification of unknown drug compounds, the *Supplemental Information* walks through three examples of how this information can used when given an unknown spectrum.

3.1.1. Barbiturates (n=10)

Barbiturates, which originally stemmed from barbituric acid (**Figure 1**), are classified as tranquilizers and are utilized for sedation and may contain substitutions at the R_1 and R_2 positions [23,25]. The compounds are not frequently observed in forensic casework – there are no barbiturates in the top 25 drugs in the NFLIS 2020 Annual report [6] or in the top reported tranquilizers.

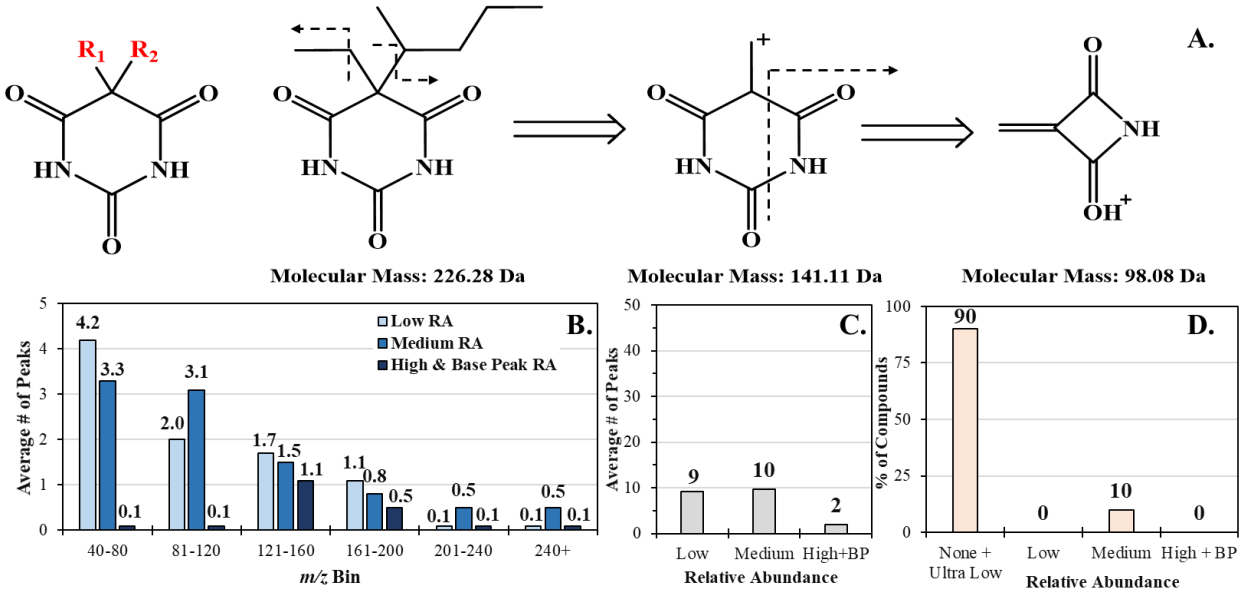

Figure 1: (A.) Core skeletal structure of barbiturates (left) and proposed fragmentation pathway of pentobarbital (right) [26–28]. (B.) Average distribution of Low (light blue), Medium (blue), and High + Base Peak (dark blue) ions across the *m/z* range, (C.) average number of peaks for each RA category (excluding *Ultra-Low*), and (D.) frequency of the presence of a molecular ion across the RA categories for the barbiturates class (n = 10).

Looking at the reoccurring ions from the 10 barbiturates in the merged database (**Table 2**), the ions at *m/z* 156, *m/z* 143, and *m/z* 168 in the *Base Peak* RA category, as well as *m/z* 41 and *m/z* 43 in the *Medium* RA category, correspond to the loss of the alkyl chain in the R_2 position. For the *High* RA category, the observed *m/z* values of *m/z* 141 and *m/z* 167 are the result of the intact ring structure but with varying *N*-alkyl chains at the R_1 and R_2 positions [26,29].

Table 2: Most frequently observed ions, neutral losses, and the total percentage of these values found in the barbiturates class (n = 10). The neutral losses represent those from *Base Peak*, *High*, and *Medium* RA ions, combined.

Base Peak RA		**High RA**		**Medium RA**		**Neutral Loss**	
m/z	**Count (%)**	***m/z***	**Count (%)**	***m/z***	**Count (%)**	**Da**	**Count (%)**
156	4 (40)	141	4 (40)	41	5 (50)	171	6 (60)
143	2 (20)	167	2 (20)	43	5 (50)	71	5 (50)
168	2 (20)			55	5 (50)	141	5 (50)
				98	4 (40)	114	4 (40)
				112	3 (30)	143	4 (40)
				157	3 (30)	183	4 (40)
				42	2 (20)	28	3 (30)
				51	2 (20)	43	3 (30)
				53	2 (20)	70	3 (30)
				56	2 (20)	85	3 (30)

From the merged database and literature reports of this limited class, potential criteria for identifying common barbiturate-related compounds include (i) lack of a molecular ion above 5% RA, (ii) presence of a peak corresponding to the fragment of the R_1 and R_2 groups which yields ions at *m/z* 41 and *m/z* 43. The remaining ring structures may have the *m/z* values in the *Base Peak* category. The *m/z* 98 ion may also be indicative as it could be a ring-closing. Common barbiturates share large peaks resembling the core ring structure followed by *Medium* RA peaks of *m/z* 41, *m/z* 43, *m/z* 55, and *m/z* 98. It is also unlikely to observe significant peaks above *m/z* 200, and the low mass range (*m/z* 40 to *m/z* 120) is dominated by *Low* and *Medium* RA peaks. Neutral losses of 171 Da, 71 Da, and 141 Da were commonly observed. Because of the small number of barbiturates in the merged database, no further conclusions are drawn.

3.1.2. Benzodiazepines (n=56)

In recent years, benzodiazepines have seen increased prevalence in casework – driven by both prescription and illicit designer compounds. The NFLIS 2020 Annual Report [6] contained four benzodiazepines in the top 25 drugs and the list of top tranquilizers is dominated by these compounds [23,30,31]. More timely resources, like NPS Discovery [7], have recently reported new benzodiazepines, such as fluclotizolam and deschloroetizolam. The general backbone of these compounds consists of the fusion of a benzene ring and a diazepine ring with various side chains of substituents (**Figure 2**). Most of the substances in this class possess di-isotopic atoms (Cl or Br) which yield unique fragmentation patterns (**Figure 2**).

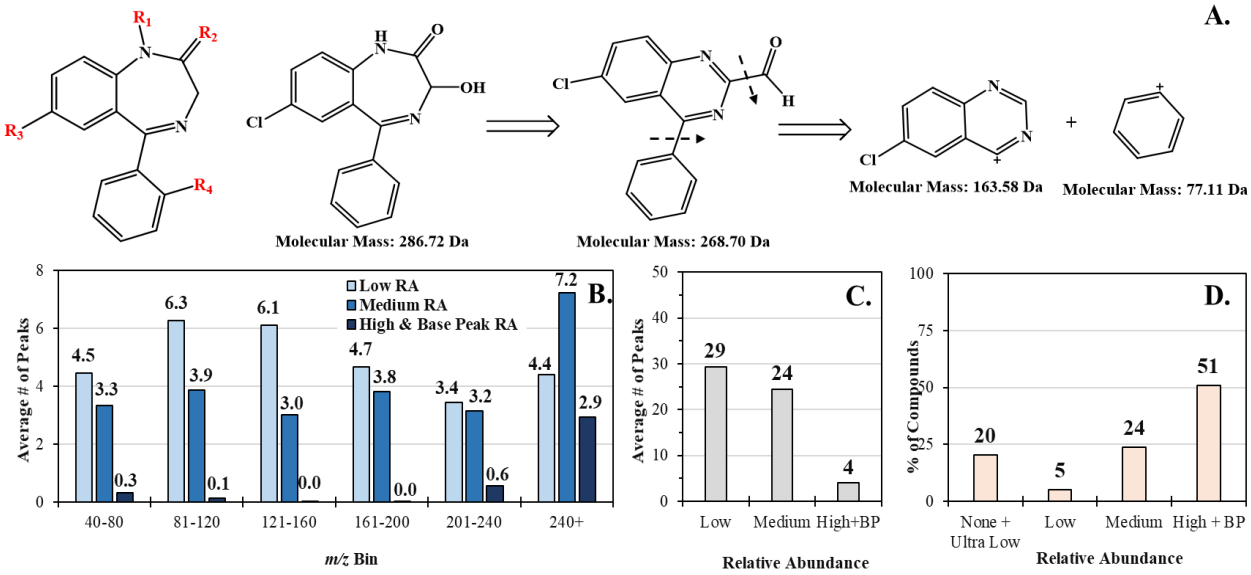

Figure 2: (A.) Core skeletal structure of benzodiazepines (left) and proposed fragmentation of oxazepam (right) [32]. (B.) Average distribution of Low (light blue), Medium (blue), and High + Base Peak (dark blue) ions across the *m/z* range, (C.) average number of peaks for each RA category (excluding *Ultra-Low*), and (D.) frequency of the presence of a molecular ion across the RA categories for the benzodiazepines class (n = 56).

For the *Base Peak* and *High* relative abundance categories in this class, most of the *m/z* values are greater than *m/z* 200 and correspond to the $M^{+}\bullet$ ion (**Figure 2**) remaining intact, and therefore are not diagnostic for class identification. Most of these structures cleave the smaller functional groups (*i.e.*, alcohols, methyl, and halogens) resulting in more high mass ions versus other classes (**Figure 2B**). Ions at *m/z* 75 and *m/z* 77 are observed across the RA categories bins (**Table 3**) and can be explained by fragmentation at the phenyl ring and the R_4 group [31,32].

Table 3: Most frequently observed ions, neutral losses, and the total percentage of these values found in the benzodiazepines class (n = 56). The neutral losses represent those from *Base Peak*, *High*, and *Medium* RA ions, combined.

Base Peak RA		High RA		Medium RA		Neutral Loss	
m/z	**Count (%)**	***m/z***	**Count (%)**	***m/z***	**Count (%)**	**Da**	**Count (%)**
205	3 (5)	75	6 (11)	75	33 (59)	29	45 (80)
286	3 (5)	77	5 (9)	102	29 (52)	27	36 (64)
75	2 (4)	288	5 (9)	177	28 (50)	28	28 (50)
204	2 (4)	269	4 (7)	51	26 (46)	63	19 (34)
222	2 (4)	286	4 (7)	163	26 (46)	26	18 (32)
223	2 (4)	287	4 (7)	76	26 (46)	35	16 (29)
259	2 (4)	294	4 (7)	89	25 (45)	104	13 (23)
267	2 (4)	315	4 (7)	63	24 (43)	119	13 (23)
275	2 (4)	203	3 (5)	77	24 (43)	43	12 (21)
283	2 (4)	239	3 (5)	151	23 (41)	189	12 (21)

The *Medium* RA category consists of ions generated from the fragmentation and recombination of the remaining core structure which can be found in numerous reports [30,33–36]. Ions at *m/z*

102, *m/z* 151, *m/z* 163, and *m/z* 177 correspond to fragmentation across the ring of various core structures. From the merged database investigation and literature reports, potential criteria for identification of novel benzodiazepines include (i) a molecular ion with at least *Medium* RA, (ii) ions at *m/z* 75 and/or *m/z* 77, (iii) mid-range RA ions indicative of the ring structure, (iv) high number of *Low* and *Medium* RA peaks spread across the mass range, and (v) few to no *High* RA peaks below *m/z* 200 . The compounds have a relatively high average number of *Low* and *Medium* RA peaks spread across the mass range and typically have no *High* RA peaks below *m/z* 200. Neutral losses of 29 Da, 27 Da, and 28 Da are common and are the result of cleaving smaller functional groups.

3.1.3. Anabolic Steroids (n=50)

Anabolic steroids are the most frequently abused substances by participants in sporting events and athletic competitions [37–39]. These compounds are not frequently observed in casework (accounting for less than 1 % of drug reports in the NFLIS 2020 Annual Report [6]) but a large range of designer steroids are observed. Newly emerging steroids that elude GC-MS identification are often modified at the 17α-position (R_2) of the ring structure of testosterone (**Figure 3**) [38]. These substances possess an alcohol or ketone in the R_2 position and when ionized, are cleaved at multiple sites.

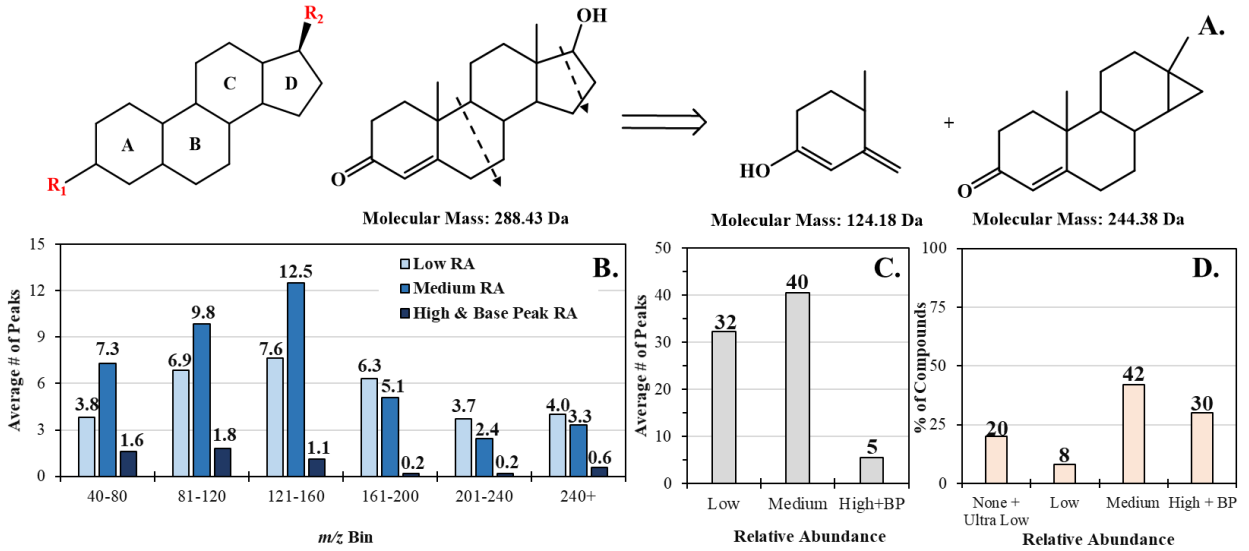

Figure 3: (A.) General structure of anabolic steroids (left) and proposed fragmentation of testosterone (right) [40]. (B.) Average distribution of *Low* (light blue), *Medium* (blue), and *High + Base Peak* (dark blue) ions across the *m/z* range, (C.) average number of peaks for each RA category (excluding *Ultra-Low*), and (D.) frequency of the presence of a molecular ion across the RA categories for the anabolic steroids class (n = 50).

Fragmentation of these molecules occurs across the entire core structure due to its relatively simplistic composition. The *Base Peak* ions at *m/z* 122 and *m/z* 124 (**Table 4)** appear to be the product ions from the B-/C-ring fragmentation (**Figure 3**) [40,41]. Out of the 50 compounds in the merged database, two compounds (Methyltestosterone and 7-keto Dehydroepiandrosterone) possessed a molecular ion of *m/z* 302 suggesting no degradation/cleavage across the B-/C-ring. Other *Base Peak* and *High* categories ions involve *m/z* 43, *m/z* 91, and *m/z* 105 which are attributed to the C-/D-ring fragmentation [42]. For the structure of *m/z* 79, it has been suggested to represent the cation of 5-methyl-cyclopenta-1,3-diene [42,43].

Table 4: Most frequently observed ions, neutral losses, and the total percentage of these values found in the anabolic steroids class (*n* = 50). The neutral losses represent those from *Base Peak*, *High*, and *Medium* RA ions, combined.

Base Peak RA		**High RA**		**Medium RA**		**Neutral Loss**	
m/z	**Count (%)**	***m/z***	**Count (%)**	***m/z***	**Count (%)**	**Da**	**Count (%)**
124	8 (16)	91	22 (44)	119	41 (82)	181	31 (62)
43	7 (14)	79	20 (40)	41	39 (78)	207	31 (62)
122	6 (12)	43	14 (28)	133	39 (78)	195	29 (58)
91	4 (8)	93	13 (26)	131	38 (76)	183	27 (54)
105	2 (4)	55	12 (24)	145	37 (78)	193	27 (54)
302	2 (4)	81	9 (18)	77	37 (74)	209	27 (54)
		147	9 (18)	121	36 (72)	171	26 (52)
		105	8 (16)	107	36 (72)	221	26 (52)
		107	8 (16)	135	36 (72)	167	25 (50)
		77	7 (14)	105	35 (71)	157	24 (48)

For the *Medium* category in **Table 4**, the top observed ions, barring *m/z* 41 and *m/z* 77, were above 100 Da and are the remaining fragmentation products of the B-/C-ring structures [41]. It is important to note that ions have been previously reported in literature as "characteristic" of anabolic steroids (*i.e., m/z* 97, *m/z* 143, *m/z* 169, and *m/z* 183) [40,42,44–49] did not appear among the top reoccurring ions observed here. From the merged database investigation and literature reports, potential criteria for identifying common performance enhancing compounds include (i) the presence of peaks at *m/z* 91, *m/z* 105, *m/z* 109, *m/z* 119, *m/z* 122, *m/z* 124, *m/z* 131, and/or *m/z* 133 at *Medium* RA or greater (ii) moderate number of peaks of *Low* and *Medium* RA that span mass range, and (iii) presence of a molecular ion, though not at a uniform intensity. There are a number of neutral losses that are common to this class including 181 Da, 207 Da, and 195 Da.

3.1.4. Cannabinoids (n=448)

Cannabinoids were first discovered from the derivation of the hemp plant *Cannabis sativa* and have been utilized for both recreational and medical purposes [50]. Cannabinoids are a structurally

diverse family of compounds and are one of the most widely abused substances [6,7,50–52]. Depending on the source (synthetic, naturally occurring, metabolism-dependent), cannabinoids can be classified into three groups: phytocannabinoids, endocannabinoids, and synthetic cannabinoids. For this study, only phytocannabinoids and synthetic cannabinoids are discussed.

3.1.4.1. Phytocannabinoids (n=24)

Phytocannabinoids are naturally occurring, plant-derived products and include Δ^9-THC, Δ^9-tetrahydrocannabivarin (Δ^9-THCV), cannabinol (CBN), cannabidiol (CBD), cannabidivarin (CBDV), cannabigerol (CBG), and cannabichromene (CBC) [53–55]. Δ^9-THC was the second most frequently reported compound in the NFLIS 2020 Annual Report, accounting for approximately 15 % of all identifications [6]. The core skeletal structure of these compounds is represented in **Figure 4** along with the common substitution sites – the isopropenyl residue at the terpenoids moiety (**1**), the resorcinol nucleus (**2**) and the alkyl side chain (**3**) [54].

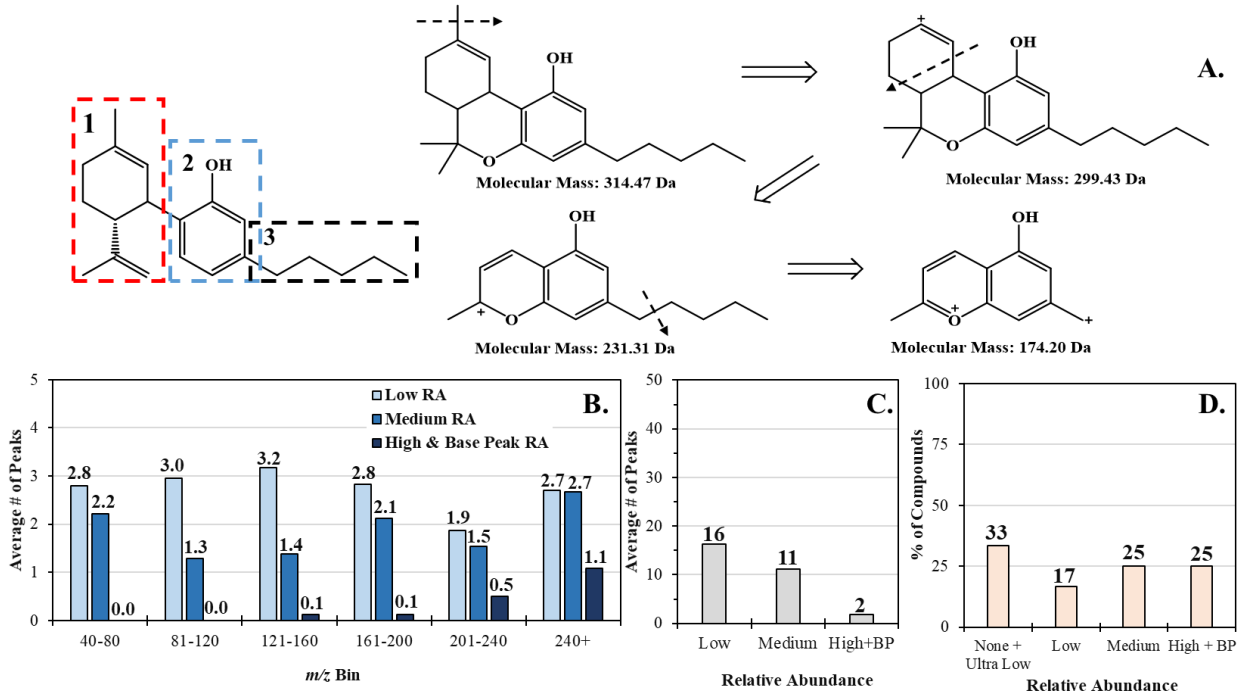

Figure 4: (A.) Core structure of the phytocannabinoids (left) outlining the terpenoids moiety (red box **1**), the resorcinol nucleus (blue box **2**) and the alkyl side chain (black box **3**) and proposed fragmentation of Δ9-THC (right) [56]. (B.) Average distribution of *Low* (light blue), *Medium* (blue), and *High + Base Peak* (dark blue) ions across the *m/z* range, (C.) average number of peaks for each RA category (excluding *Ultra-Low*), and (D.) frequency of the presence of a molecular ion across the RA categories for the phytocannabinoids class (*n* = 24).

Roughly 29 % of the compounds in this class displayed a *Base Peak* at *m/z* 231 (**Table 5**) which can be attributed to structural similarities at the resorcinol nucleus (**B**) and the 5-alkyl side chain (**C**) [57,58]. The remaining ions in the *Base Peak* category are caused by fragmentation

occurring at the terpenoids moiety or along the alkyl side chain. This observation remains consistent for the ions in the *High* RA category as the substitutions become bulkier [59].

Table 5: Most frequently observed ions, neutral losses, and the total percentage of these values found in the phytocannabinoids class (n = 24). The neutral losses represent those from *Base Peak*, *High*, and *Medium* RA ions, combined.

Base Peak RA		**High RA**		**Medium RA**		**Neutral Loss**	
m/z	**Count (%)**	***m/z***	**Count (%)**	***m/z***	**Count (%)**	**Da**	**Count (%)**
231	7 (29)	299	3 (13)	174	16 (67)	83	16 (67)
137	2 (8)	314	3 (13)	41	14 (58)	68	9 (38)
203	2 (8)	271	2 (8)	43	9 (38)	43	8 (33)
313	2 (8)			232	9 (38)	15	7 (29)
				91	9 (38)	85	6 (25)
				77	8 (33)	121	6 (25)
				69	7 (29)	140	5 (21)
				175	6 (25)	112	4 (17)
				79	6 (25)	127	4 (17)
				260	6 (25)	141	4 (17)

With the *Medium* category, the *m/z* 174 ion is the most frequently observed and corresponds to the fragmentation of the alkyl side chain [57]. Other common ions such as *m/z* 41, *m/z* 43, *m/z* 232, and *m/z* 91 correspond to fragments of the core structure containing the aromatic ring. The observations of these ions are also documented frequently throughout various literature reports [50,60,61]. From the merged database investigation and literature reports, potential criteria for identifying common phytocannabinoids include (i) the presence of ions at *m/z* 231/232, *m/z* 313/314, and *m/z* 174, (ii) a number of *Low* and *Medium* RA peaks across the *m/z* range, and (iii) a limited number of *High* RA peaks. Neutral losses of 83 Da and 68 Da are common. Due to the wide variety of core structures, the presence and RA of a molecular ion is inconsistent.

3.1.4.2. Synthetic Cannabinoids (n=424)

Synthetic cannabinoids (SCs) such as “Spice”, “K2”, and “Joker”, have often eluded efforts to be regulated due to slight structural modifications [62]. According the NFLIS 2020 Annual Report, synthetic cannabinoids account for approximately 1 % of all identifications [6], which are spread across many different compounds and core structures (**Figure 5**). New synthetic cannabinoids are frequently reported by groups such as NPS Discovery, who reported ten new compounds in 2021 alone [7].

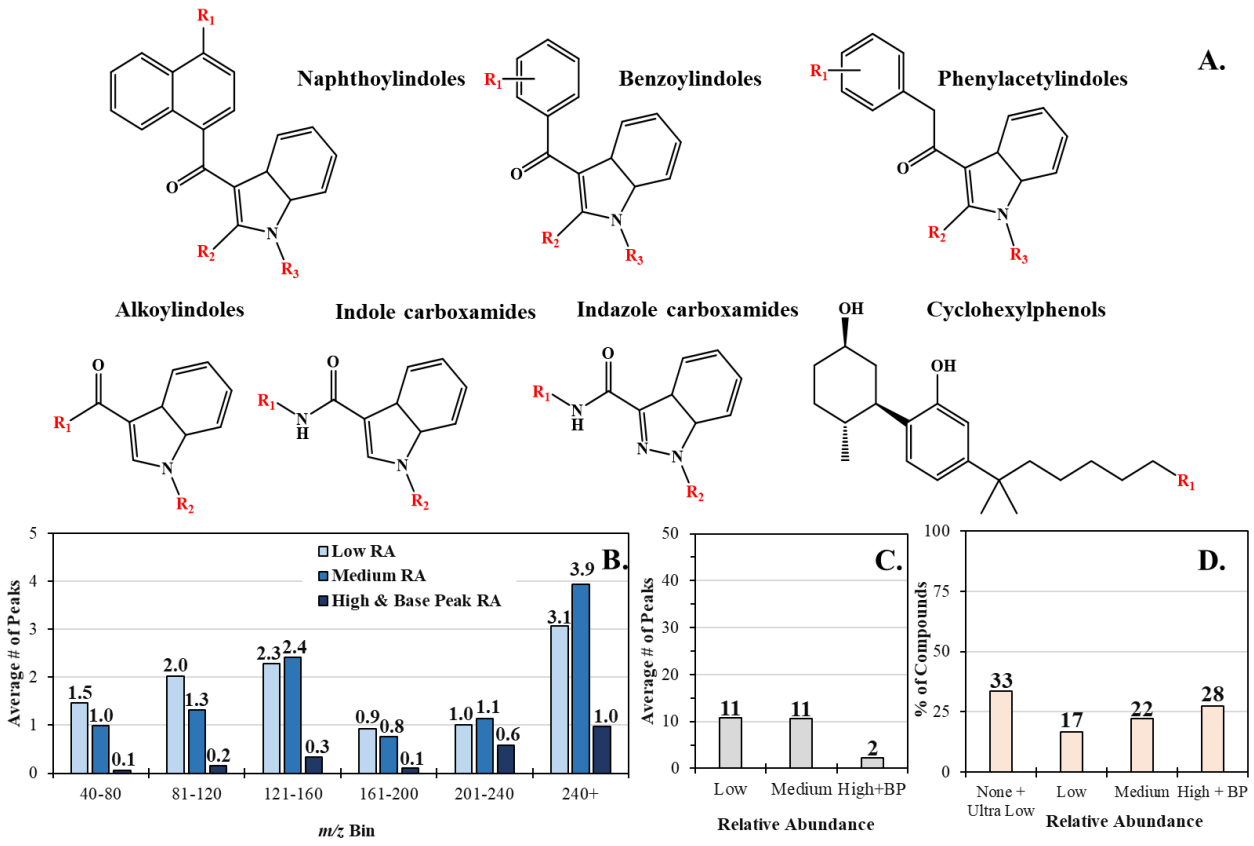

Figure 5: (A.) Reported core structures of synthetic cannabinoids [63]. (B.) Average distribution of *Low* (light blue), *Medium* (blue), and *High + Base Peak* (dark blue) ions across the *m/z* range, (C.) average number of peaks for each RA category (excluding *Ultra-Low*), and (D.) frequency of the presence of a molecular ion across the RA categories for the synthetic cannabinoids class (n = 424).

Within this diverse subclass, however, there are a few notable trends between compounds across the RA categories. For instance, the *Base Peaks* at *m/z* 214 and *m/z* 232 have a core structure attributed to a non-fluorinated versus a fluorinated ion, respectively, formed by fragmentation between the carbonyl carbon and benzyl carbon (*i.e.*, the alpha carbon) with one electron going into the indole-carbonyl system and the other electron forming the methoxybenzyl radical leaving group [64,65]. For the ions at *m/z* 215 and *m/z* 233, most of the core structures resemble the alkylindoles, indole, and carboxamides, barring substances similar to 3-epi CP 47,497 which has a core structure of cyclodexylphenols.

Table 6: Most frequently observed ions, neutral losses, and the total percentage of these values found in the synthetic cannabinoids class (n = 424). The neutral losses represent those from *Base Peak*, *High*, and *Medium* RA ions, combined.

Base Peak RA		**High RA**		**Medium RA**		**Neutral Loss**	
m/z	**Count (%)**	***m/z***	**Count (%)**	***m/z***	**Count (%)**	**Da**	**Count (%)**
232	47 (11)	127	27 (11)	144	187 (44)	57	87 (21)
214	44 (10)	145	21 (3)	116	112 (26)	17	84 (20)

233	31 (7)	284	20 (3)	41	106 (25)	71	67 (16)
109	29 (7)	144	18 (4)	254	93 (22)	127	63 (15)
215	21 (5)	155	18 (4)	128	88 (21)	15	61 (14)
127	14 (3)	298	14 (3)	43	83 (16)	186	58 (14)
284	11 (3)	253	14 (3)	241	75 (16)	214	56 (13)
100	10 (3)	214	13 (3)	115	72 (16)	85	47 (11)
241	8 (2)	232	11 (3)	145	70 (16)	144	47 (11)
355	8 (2)	341	10 (3)	270	70 (11)	115	44 (10)

For core structures similar to naphthoylindoles, benzoylindoles, and phenylacetylindoles, the common fragment ion of *m/z* 144 may form by a 1,3-hydride transfer from the alkyl carbon between the nitrogen and the alkyl group (R_3), forming a π-bond on the pentene leaving group [64]. Additionally, the *m/z* 109 ion has been recorded to be characteristic of fluorine-containing synthetic cannabinoids [66].

For structures that are similar in structure to the indole and carboxamide (*i.e.*, AB-PINACA and AB-CHMINACA), the common fragment ions of *m/z* 145 and *m/z* 241 are observed which can be attributed to the main core structure [66–70]. Simple cyclohexylphenols structures (*i.e.*, CP-47497) exhibit similar fragments like *m/z* 215 and *m/z* 233 [71]. With the merged database investigation and literature reports, potential criteria for identification of synthetic cannabinoids include (i) presence of *m/z* 109, *m/z* 116/117, *m/z* 144/145, *m/z* 214/215, *m/z* 232/233, and *m/z* 241 [72–75], (ii) *Low* and *Medium* RA peaks, a majority of which are at *m/z* values greater than 240, and (iii) few to no *High* RA peaks below *m/z* 200. The presence and RA of a molecular ion is inconsistent across this class. Some common neutral loss ions include 57 Da, 17 Da, and 71 Da.

3.1.5. Opioids (n=323)

Opiates, which are based on the alkaloids extracted from the poppy seed, contain both natural and semi-synthetic compounds. Heroin, buprenorphine, and oxycodone are frequently observed opiates in casework, represent the 5th, 7th, and 8th most frequently reported compounds in the NFLIS 2020 Annual Report – accounting for approximately 10 % of all drug identifications [6].

3.1.5.1. Opiates (n=36)

With the initial extraction from the poppy seed, researchers identified the main alkaloids responsible for its pharmacologic effects [76]. These compounds are mainly used to mitigate pain by activating receptors in the brain to release endorphins and thus, depressing the central nervous system [6,76–78]. However, opiates were overshadowed by the development of heroin, a semi-

synthetic opiate, which exhibits a similar core structure to morphine but with the addition of two acetyl groups.

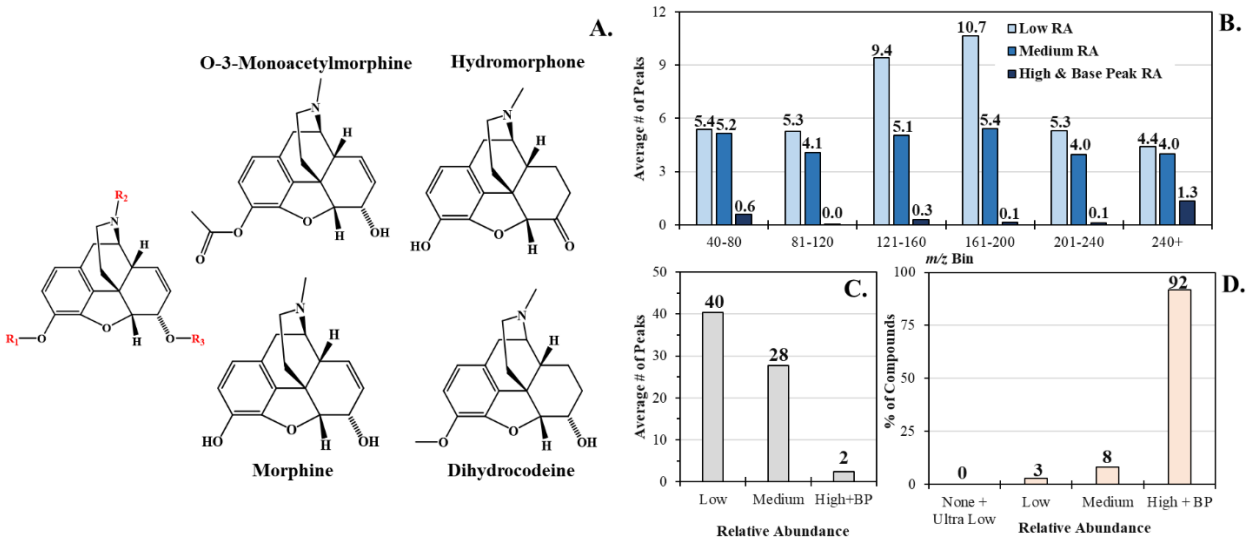

Figure 6: (A.) Core structure of opiates (left) and structural similarities amongst a subset of these substances (right). (B.) Average distribution of *Low* (light blue), *Medium* (blue), and *High + Base Peak* (dark blue) ions across the *m/z* range, (C.) average number of peaks for each RA category (excluding *Ultra-Low*), and (D.) frequency of the presence of a molecular ion across the RA categories for the opiates class (n = 36).

Most of the opiates within this class have similar core structures (**Figure 6**) with substitutions commonly found at the R_1 and R_3 groups. Looking at the merged database information, the *Base Peak* and *High* RA categories contain multiple ions which correspond to the molecular ions. From these two categories, *m/z* 285 and *m/z* 42 are equally observed ions which are attributed to the fused-ring core structure and fragments of smaller functional groups.

Table 7: Most frequently observed ions, neutral losses, and the total percentage of these values found in the opiates class (n = 36). The neutral losses represent those from *Base Peak*, *High*, and *Medium* RA ions, combined.

Base Peak RA		High RA		Medium RA		Neutral Loss	
m/z	**Count (%)**	***m/z***	**Count (%)**	***m/z***	**Count (%)**	**Da**	**Count (%)**
285	5 (14)	42	5 (14)	115	31 (86)	57	16 (44)
301	4 (11)	55	3 (8)	128	30 (83)	85	14 (39)
303	3 (8)	70	3 (8)	77	24 (67)	259	14 (39)
317	3 (8)	162	3 (8)	127	22 (61)	87	13 (36)
287	2 (6)	216	3 (8)	44	22 (61)	101	13 (36)
299	2 (6)	327	3 (8)	91	21 (58)	128	13 (36)
343	2 (6)	43	2 (6)	42	20 (55)	100	12 (33)
		150	2 (6)	70	18 (50)	116	12 (33)
		157	2 (6)	200	17 (47)	245	12 (33)
		256	2 (6)	131	17 (47)	17	11 (31)

Within the *Medium* RA category, ions at *m/z* 115 and *m/z* 128 occur in over 80 % of the compounds. Interestingly, there have been few reports suggesting the structures of these ions, but

those that do exist attribute their formation to the loss of larger neutral fragments [79–81]. From the merged database investigation, potential criteria for identifying common opiates include (i) a molecular ion with a high RA, (ii) ions at *m/z* 115 and/or *m/z* 128, and (iii) a high number of *Low* and *Medium* RA ions spread across the *m/z* range. Neutral losses of 57 Da, 85 Da, and 259 Da are common.

3.1.5.2. Fentanyls (n=237)

The rise, and continued prevalence, of fentanyl in casework has been well documented [6]. Fentanyl is the fourth most frequently reported drug in the NFLIS 2020 Annual Report, accounting for 9 % of all identifications [6]. While the number of fentanyl analogs reported has dropped, new analogs, such as fluorofentanyl, bromofentanyl, and chlorofentanyl are still to be identified [7]. The core structure of fentanyl is illustrated in **Figure 7** to which common substitutions occur at the amide (R_1), aniline (R_2), piperidine (R_3), and phenethyl chain (R_4) groups [82].

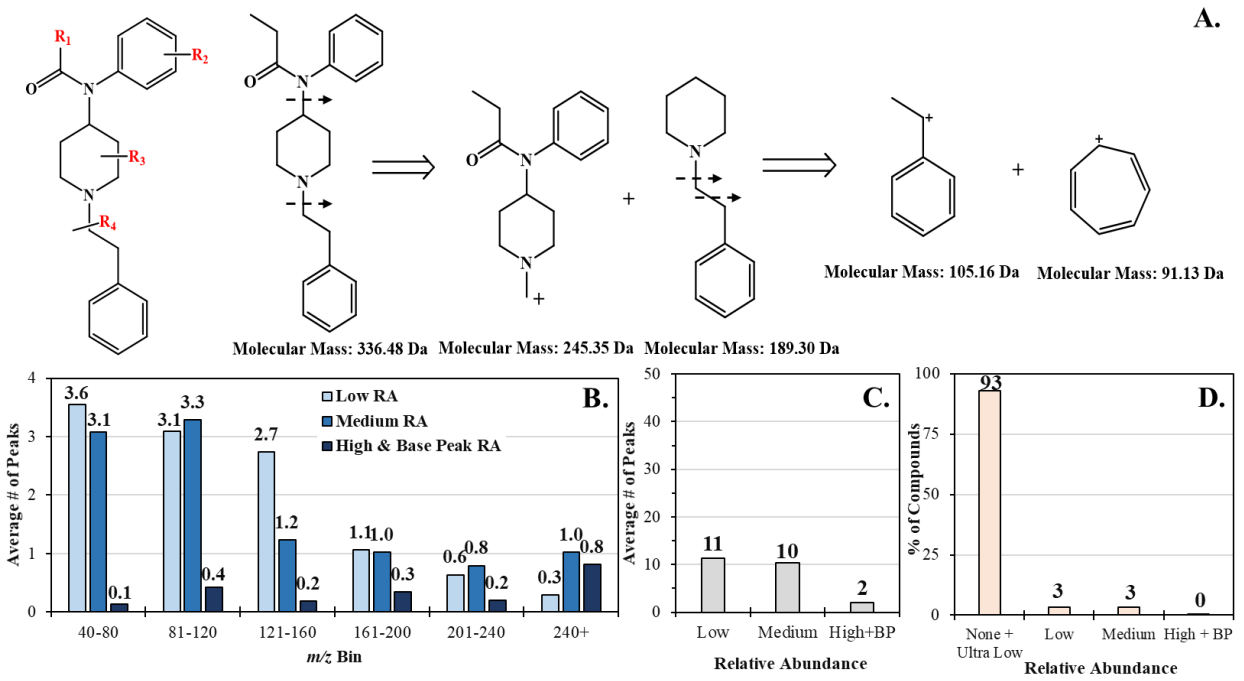

Figure 7: (A.) Base skeletal structure of fentanyl (left) and proposed fragmentation of a few key structures (right) [82,83]. (B.) Average distribution of *Low* (light blue), *Medium* (blue), and *High + Base Peak* (dark blue) ions across the *m/z* range, (C.) average number of peaks for each RA category (excluding *Ultra-Low*), and (D.) frequency of the presence of a molecular ion across the RA categories for the fentanyl class (n = 237).

This subclass posseses a few notable trends between compounds across the RA categories. For instance, the frequently observed *Base Peaks* at *m/z* 245 and *m/z* 259 differ by 14 Da which, structurally, correspond to the presence of a methyl group on the fragment ion caused by breaking the phenethyl chain and piperidine. The compounds found with these ions share a core similarity

to fentanyl whereas the structures that generate an *m/z* 91 ion are replaced via a N-benzyl or N-methyl moiety [84–86]. For compounds with an ion at *m/z* 95 (**Table 8)**, cleavage occurs along the amide C-N bond correlating to resonance-stabilization of the R_1 functional group (*i.e.*, 2-Furanyl fentanyl).

Table 8: Most frequently observed ions, neutral losses, and the total percentage of these values found in the fentanyl class (*n* = 237). The neutral losses represent those from *Base Peak*, *High*, and *Medium* RA ions, combined.

Base Peak RA		**High RA**		**Medium RA**		**Neutral Loss**	
m/z	**Count (%)**	***m/z***	**Count (%)**	***m/z***	**Count (%)**	**Da**	**Count (%)**
245	36 (15)	146	31 (13)	42	173 (73)	91	140 (59)
259	25 (11)	160	19 (8)	96	152 (64)	134	74 (31)
91	16 (7)	82	13 (6)	91	148 (62)	259	45 (19)
95	15 (6)	189	12 (5)	105	137 (58)	204	43 (18)
277	15 (6)	164	10 (4)	77	107 (45)	293	43 (18)
273	10 (4)	203	9 (4)	57	76 (32)	279	38 (16)
231	8 (3)	69	8 (3)	146	71 (30)	245	37 (16)
275	8 (3)	96	7 (3)	132	58 (24)	190	32 (14)
83	7 (3)	105	7 (3)	189	54 (15)	297	32 (14)
271	7 (3)	176	5 (2)	41	45 (15)	307	32 (14)

For the *High* RA category, the ions at *m/z* 146 and *m/z* 189 reveal compounds with no substitution of the aniline (R_2) or piperidine (R_3) regions. These ions also appear in the *Medium* RA category (**Table 8)** along with *m/z* 42, *m/z* 96, *m/z* 91, and *m/z* 105 which are also reported in literature [15,82,83,87,88]. An ion at *m/z* 96, can occur for a variety of reasons including the isotope of a *m/z* 95 *Base Peak* (*i.e.*, furanyl fentanyl and its analogs) [89] or as the fragmentation of the piperidine ring (suggested by *NIST MS Interpreter* tool). For the ions at *m/z* 42, *m/z* 91, and *m/z* 105, there are a variety of reports that depict the formation of these ions as fragmentation of the pyridine ring, the tropylium ion, and a methyl-substituted tropylium ion, respectively [12,77,82,83,87,90,91]. From the merged database investigation and literature reports, potential criteria for identifying common fentanyl-related compounds include (i) the presence of ions at *m/z* 245 or *m/z* 259 as well as *m/z* 91 and *m/z* 105, (ii) lack of an appreciable (> 5 % RA) molecular ion, and (iii) spectra dominated by *Low* and *Medium* RA peaks below *m/z* 160. Neutral losses of 91 Da and 134 Da are common. It should be noted that tools exist for the determination potential structures of novel fentanyls [11].

3.1.5.3. Utopiods (n=35)

In conjunction with fentanyl-related cases, other new synthetic opioids (NSO) have risen within the past decade [4,5,92]. Many of these initial cases reported U-47700, however, an influx

of other U-compounds (U-51754, U-49900, U-48800, etc.) started to appear to elude legislature once U-47700 was scheduled [93]. While the U-series compounds are not among the most frequently reported drugs, new U-compounds (such as trifluoromethyl-U-47700 and naphthyl-U-47700) have been reported recently. The core structure of this subclass is illustrated in **Figure 8** and is generally substituted on the phenyl ring (R_4), the amine group (R_3), or the amine group on the cyclohexane ring (R_1 and R_2) [92].

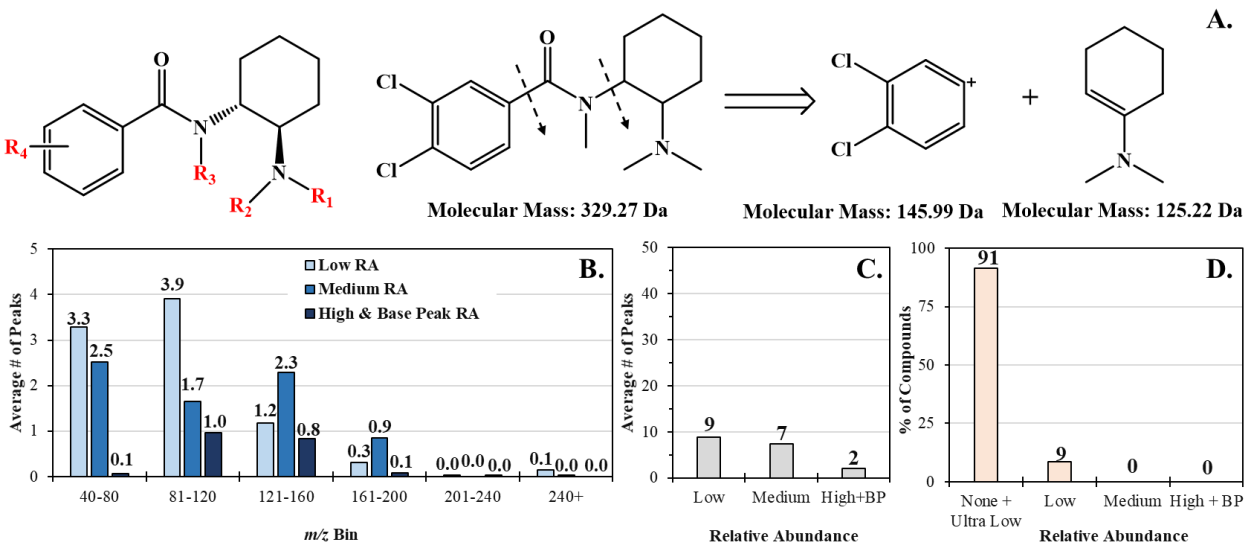

Figure 8: (A.) General structure of utopioids (left) and proposed fragmentation of U-47700 (right) [94]. (B.) Average distribution of *Low* (light blue), *Medium* (blue), and *High + Base Peak* (dark blue) ions across the *m/z* range, (C.) average number of peaks for each RA category (excluding *Ultra-Low*), and (D.) frequency of the presence of a molecular ion across the RA categories for the utopioids class (n = 35).

Although the merged database contains only 35 compounds, there are still notable trends for these compounds. Across the *Base Peak* and *High* categories (**Table 9**), ions at *m/z* 84 and *m/z* 125 (present in 77 % and 69 % of compounds, respectively) relate to the *N*, *N*-dimethylcyclohexanamine fragment (**Figure 8**) [95]. The *m/z* 125 ion is caused by cleaving the bond between the amide moiety and the cyclohexane [96,97]. The fragmentation pathway for the generation of the *m/z* 84 ion has not been proposed. Using the *NIST MS Interpreter* tool, one potential pathway involves EI fragmentation occurs across the cyclohexane ring while maintaining the amide group. The remaining *m/z* values in this category correspond to compounds with varying methyl groups that still fragment at the amide moiety–cyclohexane bond.

The *NIST MS Interpreter* tool was used to understand the fragmentation of the remaining *High* RA category ions. For the *m/z* 70 ion, fragmentation across the cyclohexane for 3,4-Difluoro-*N*-desmethyl U-47700 and *N*-Desmethyl U-47700 was suggested. The *m/z* 141 ion appears to be

generated by fragmenting the amine and carbonyl groups on 3,4-Difluoro-N-desmethyl U-47700 and 3,4-Difluoro Isopropyl U-47700. For the *Medium* RA category, ions at *m/z* 58 and *m/z* 71 occur in over 70 % of the compounds and suggest the dissociation from the cyclohexane and a 1,2 dissociation of the cyclohexane ring.

Table 9: Most frequently observed ions, neutral losses, and the total percentage of these values found in the utopioids class (*n* = 35). The neutral losses represent those from *Base Peak*, *High*, and *Medium* RA ions, combined.

Base Peak RA		**High RA**		**Medium RA**		**Neutral Loss**	
m/z	**Count (%)**	***m/z***	**Count (%)**	***m/z***	**Count (%)**	**Da**	**Count (%)**
84	19 (54)	125	18 (51)	71	26 (74)	183	20 (57)
125	6 (17)	84	8 (23)	58	25 (71)	218	10 (29)
111	3 (9)	70	2 (6)	124	24 (69)	244	10 (29)
112	2 (6)	141	2 (6)	110	20 (57)	155	9 (26)
				42	19 (54)	181	8 (23)
				173	10 (23)	186	7 (20)
				145	10 (29)	211	7 (20)
				147	9 (26)	240	7 (20)
				175	8 (23)	169	6 (17)
				126	8 (23)	203	6 (17)

Interestingly, many of these compounds possess halogens on the aromatic ring (R_4) yielding distinct isotopic distributions. There are several compounds in this class that have two chlorine atoms (Cl) present, creating a unique isotopic pattern consisting of three peaks, each separated by 2 Da with the ratio of 100:63.9:10.2 [21]. An example of this pattern is observed in U-47700 at *m/z* 145, *m/z* 147, and *m/z* 149 which corresponds to the benzene ring containing both chlorine atoms. From the merged database analysis and literature reports, potential criteria for identifying U-series compounds include (i) ions at *m/z* 84, *m/z* 125, *m/z* 58, and/or *m/z* 71, (ii) lack of an appreciable (>5 % RA) molecular ion, and (iii) a number of *Low* and *Medium* RA peaks below *m/z* 160. Common neutral losses include 183 Da, 218 Da, and 244 Da.

3.1.5.4. Nitazenes (n=15)

Contributing to the surge of synthetic opioids is a new class of compounds commonly referred to as "nitazenes". Like the Utopioids, nitazenes are not among the most frequently observed compounds but the continued detection of new compounds in case in recent months (such as N-piperidinyl etonitazene and metonitazene) has been reported [98]. The core structure of these compounds has three substitution regions (**Figure 9**) located on the aminoethyl chain (R_1), the benzimidazole core (R_2), and the connected benzyl moiety (R_3).

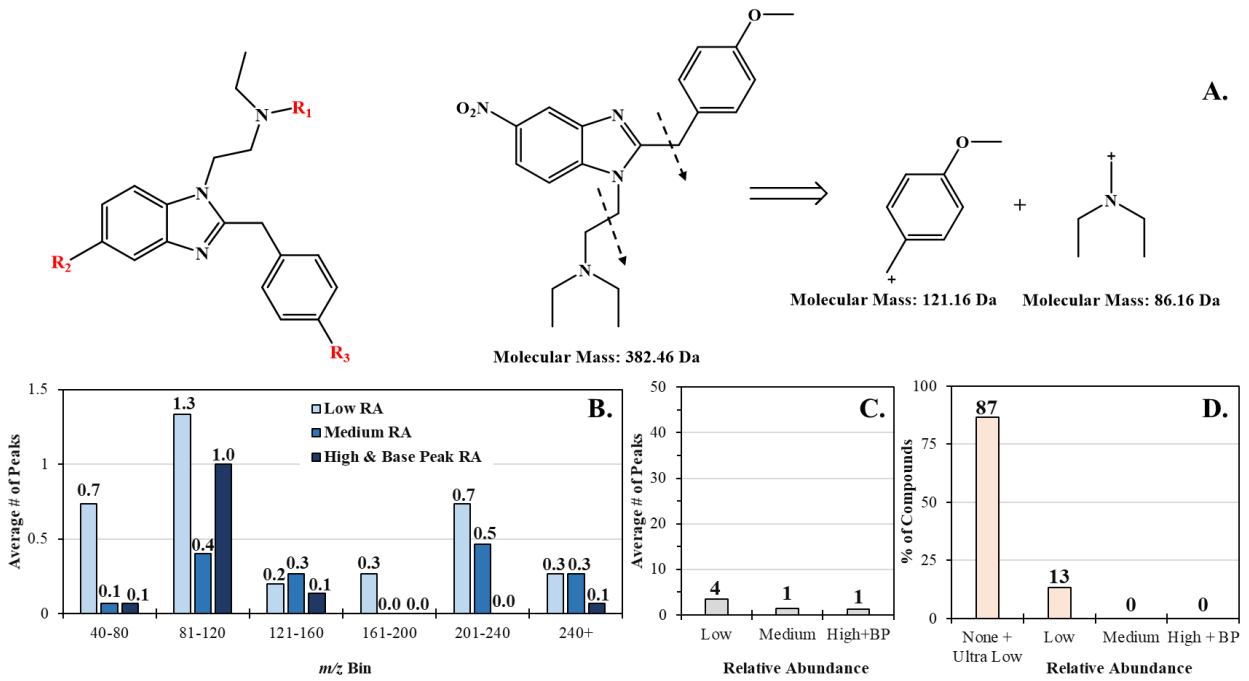

Figure 9: (A.) General core structure of the nitazenes compounds (left) and proposed fragmentation of metonitazene (right) [98]. (B.) Average distribution of *Low* (light blue), *Medium* (blue), and *High + Base Peak* (dark blue) ions across the *m/z* range, (C.) average number of peaks for each RA category (excluding *Ultra-Low*), and (D.) frequency of the presence of a molecular ion across the RA categories for the nitazenes class (n = 15).

The mass spectra of the nitazenes possess several noteworthy ions (**Table 10**). An ion at *m/z* 86 occurs as the *Base Peak* in 80 % of the substances, corresponding to the fragmentation (**Figure 9**) of diethyl aminoethyl moiety (R_1). The three compounds that do not possess this fragment ion (*N*-Desethyl Isotonitazene, *N*-Pyrrolidino Etonitazene, *N*-Desethyl Etonitazene) have *Base Peaks* at *m/z* 149, *m/z* 84, and *m/z* 135, respectively, which can be attributed to varying substitutions at the R_1 moiety.

Table 10: Most frequently observed ions, neutral losses, and the total percentage of these values found in the nitazenes class (n = 15). The neutral losses represent those from *Base Peak*, *High*, and *Medium* RA ions, combined.

Base Peak RA		High RA		Medium RA		Neutral Loss	
m/z	**Count (%)**	***m/z***	**Count (%)**	***m/z***	**Count (%)**	**Da**	**Count (%)**
86	12 (80)	107	5 (33)	87	12 (80)	261	5 (33)
		207	3 (20)	107	6 (40)	310	4 (27)
		121	2 (13)	58	5 (33)	324	3 (20)
		235	2 (13)	77	3 (20)	57	2 (13)
						130	2 (13)
						233	2 (13)

The second frequently encountered fragment, *m/z* 107, corresponds to the benzyl moiety (R_3) with an ether group while the ions at *m/z* 207 and *m/z* 235 correspond to the resulting benzimidazole core (R_2) with the difference of an ethyl substitution [99]. Other frequently observed ions at (i) *m/z*

87, (ii) *m/z* 58, and (iii) *m/z* 77 are formed from (i) the natural isotope of *m/z* 86, (ii) fragmentation of the diethyl aminoethyl fragment (R_1), and (iii) the resulting phenyl ring fragment of the benzyl moiety (R_3). From the limited research [14,98,100] along with this merged database investigation, potential characteristic ions for nitazenes include (i) ions at *m/z* 86 and *m/z* 107, (ii) an overall feature poor spectrum containing few peaks, (iii) lack of an appreciable (>5 % RA) molecular ion, and few, if any, ions above *m/z* 120. Common neutral losses observed are 261 Da and 310 Da.

3.1.6. Stimulants (n=600)

Stimulants represent a wide range of compounds that are used to create feelings of euphoria. These compounds are amongst the most frequently encountered in forensic casework and recent reports have indicated that an increase in overdoses may be coming, involving stimulant use in combination with fentanyl-related compounds [1,101,102].

3.1.6.1. Cathinones (n=229)

Among this new wave of stimulants are the synthetic cathinones which are often labelled as "bath salts", "plant food", or "insect repellant" to elude law enforcement [103–105]. Eutylone is the only cathinone listed on the NIFLIS 2020 Annual Report as a top 25 reported drug (9^{th} on the list, compromising 1 % of all identifications [6]) but, like synthetic cannabinoids, there are a wide range of these novel compounds that have been identified in casework [6]. Generally, synthetic cathinones have several substitution locations on the core structure (**Figure 10**) including the benzyl moiety (R_1), the α-alkyl carbon (R_2), and the amino group (R_3 and R_4). The EI mass spectra of synthetic cathinones are dominated by the formation of iminium and acylium ions and readily dissociate at the α and β-carbon bond [106–108].

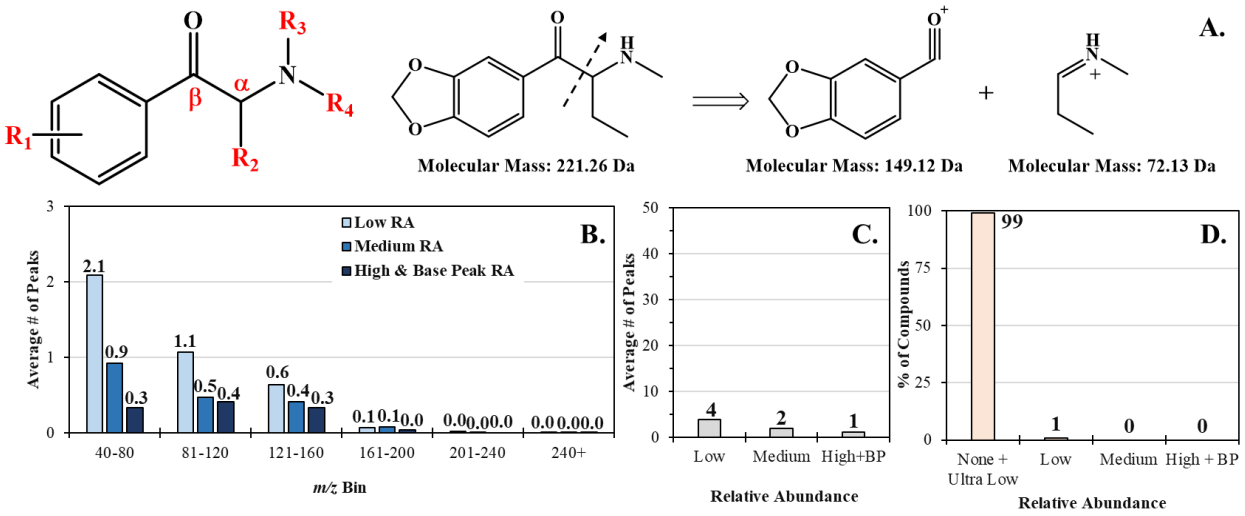

Figure 10: (A.) General core structure of synthetic cathinones (left) and proposed fragmentation of butylone (right) [3]. (B.) Average distribution of *Low* (light blue), *Medium* (blue), and *High + Base Peak* (dark blue) ions across the *m/z* range, (C.) average number of peaks for each RA category (excluding *Ultra-Low*), and (D.) frequency of the presence of a molecular ion across the RA categories for the cathinones class (n = 229).

For the cathinones, it has been reported that base peak ions of *m/z* 58, *m/z* 72, *m/z* 86, or *m/z* 100 (**Table 11**), represent fragment ions corresponding to varying alkyl chain lengths in the R_3 substitution [108]. This observation is consistent with what was observed in the merged database.

Table 11: Most frequently observed ions, neutral losses, and the total percentage of these values found in the cathinones class (n = 229). The neutral losses represent those from *Base Peak*, *High*, and *Medium* RA ions, combined.

Base Peak RA		High RA		Medium RA		Neutral Loss	
m/z	**Count (%)**	***m/z***	**Count (%)**	***m/z***	**Count (%)**	**Da**	**Count (%)**
72	36 (16)	134	4 (2)	44	41 (18)	149	49 (21)
58	30 (13)			77	36 (16)	105	36 (16)
86	25 (11)			95	22 (10)	119	35 (15)
100	23 (10)			65	20 (9)	123	22 (10)
126	23 (10)			56	20 (9)	128	22 (10)
140	14 (6)			91	20 (9)	100	21 (9)
128	13 (6)			58	19 (8)	133	21 (9)
112	11 (5)			149	18 (8)	114	19 (8)
98	10 (4)			127	16 (7)	161	17 (7)
114	8 (4)			75	14 (6)	139	16 (7)

The mass spectra for the cathinones consist of one base peak followed by a few medium peaks. In addition to the previously mentioned *m/z* values, there are trends with regards to ions at *m/z* 98, *m/z* 112, *m/z* 126, and *m/z* 140. For the compounds that exhibit these *m/z* values, the amino fragment is instead substituted by a pyrrolidine moiety. Within the *Medium* RA category, *m/z* values of *m/z* 44 and *m/z* 77 correspond to minimal or no substitutions on the amino group and the aromatic rings, respectively. From the published literature along with this merged database investigation, potential criteria for the identification of cathinones include (i) *Base* and *High* RA

ions at *m/z* 58, *m/z* 72, *m/z* 86 and *m/z* 100, (ii) along with *Medium* RA ions of *m/z* 44 and *m/z* 77, (iii) feature-poor spectra dominated with ions. Spectra of these compounds often have few peaks of appreciable intensity and those that are present are typically below *m/z* 120, and (iv) lack of an appreciable (> 5 % RA) molecular ion. Common the neutral losses include 149 Da, 105 Da, and 119 Da.

3.1.6.2. Amphetamines (n=174)

One of the most abused compound classes to date is the amphetamine derivatives class which had a global seizure of 144,000 kg (144 tons) between 2003 and 2012 [109]. Methamphetamine was the most frequently reported drug in the NFLIS 2020 Annual Report (29 % of all identifications). Amphetamine and 3,4-methylenedioxy-N-methylamphetamine (MDMA) are also frequently encountered compounds [110]. The core structure of the amphetamines is derived from phenethylamine, represented in **Figure 11**, and can be substituted on the phenyl ring (R_1), the amino group, and the alkyl chain.

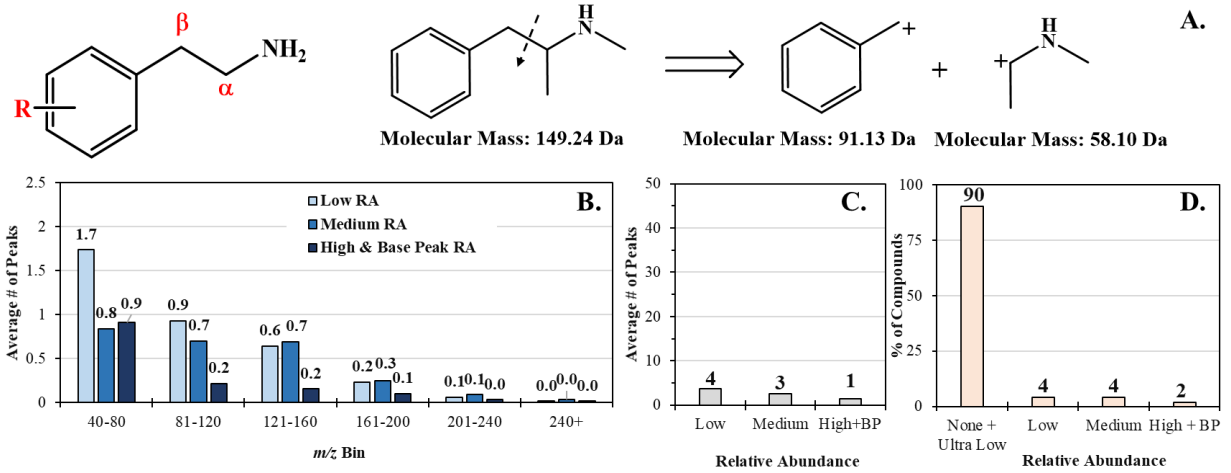

Figure 11: (A.) Core structure derived from phenethylamine (left) and proposed fragmentation of methamphetamine (right) [111]. (B.) Average distribution of *Low* (light blue), *Medium* (blue), and *High + Base Peak* (dark blue) ions across the *m/z* range, (C.) average number of peaks for each RA category (excluding *Ultra-Low*), and (D.) frequency of the presence of a molecular ion across the RA categories for the amphetamines class (*n* = 174).

Under EI conditions, amphetamines readily dissociate at the α and β-carbon bond, resulting in simple, feature-poor, mass spectra. The mass spectra for these compounds often exhibit a *Base Peak* with up to one additional *High* RA peak and a small number of *Medium* and *Low* RA peaks.

Some frequent ions identified by the merged database investigation and literature values are *m/z* 44, *m/z* 58, and *m/z* 72 which are comprised of the fragmentation of the α and β-carbon bond and the resulting in the amino groups (**Figure 11**) [109,112,113]. Out of the 174 compounds in the

merged database, these three ions account for approximately 69 % of all *Base Peaks* observed (**Table 12**).

Table 12: Most frequently observed ions, neutral losses, and the total percentage of these values found in the amphetamines class (n = 174). The neutral losses represent those from *Base Peak*, *High*, and *Medium* RA ions, combined.

Base Peak RA		**High RA**		**Medium RA**		**Neutral Loss**	
m/z	**Count (%)**	***m/z***	**Count (%)**	***m/z***	**Count (%)**	**Da**	**Count (%)**
44	58 (33)	44	7 (4)	77	32 (18)	43	43 (25)
58	43 (25)	91	6 (3)	91	29 (17)	58	29 (17)
72	19 (11)	43	3 (2)	44	21 (12)	44	24 (14)
86	5 (3)	166	3 (2)	65	16 (9)	91	22 (13)
91	5 (3)	102	2 (1)	89	16 (9)	72	21 (12)
84	4 (2)	130	2 (1)	131	15 (9)	131	16 (9)
100	2 (1)	135	2 (1)	151	13 (7)	135	15 (9)
116	2 (1)	149	2 (1)	135	10 (6)	151	15 (9)
118	2 (1)	150	2 (1)	90	9 (5)	100	12 (12)
121	2 (1)	164	2 (1)	63	9 (5)	86	11 (6)

Aside from these ions, as well as *m/z* 77 and *m/z* 91, the rest of the ions are largely specific to unique subsets of compounds (**Figure 11**). From the literature [110,112,113] and merged database investigation, potential criteria for identification of amphetamines include (i) ions at *m/z* 44, *m/z* 58, *m/z* 72, and *m/z* 91, (ii) spectra with one or two *Base* or *High* peaks and relative few *Medium* or *Low* RA peaks, (iii) spectral where nearly all of the peaks are below *m/z* 160, and (iv) lack of an appreciable (>5 % RA) molecular ion. Common neutral losses are 43 Da and 58 Da.

3.1.6.3. Phenethylamines (n=127)

Phenethylamines are another class of compounds increasingly being observed in casework that, like synthetic cannabinoids, have a wide range of core structures. These core structures include amphetamine-like, “2C”-series, “D”-series, “NBOMe”-series, “FLY”- series, and “DRAGONFLY”-series compounds [114–118]. These molecules sub-groups are based on the different substitutions found on the aromatic ring (R_1), on the α and β-carbon alkyl chain (R_α and R_β), or on the nitrogen atom (R_N) (**Figure 12**).

The core phenethylamine structure is primarily preserved in the amphetamine-like compounds with simple substitutions on the R_α or on the phenyl group (observed with MDMA). More complex structures were synthesized on the phenyl group with the introduction of the “2C”-series where there are two methoxy groups on the 2- and 5- positions [119]. The “D”-series consists of two methoxy groups on the phenyl ring, and a single substituent on the 4- position of the phenyl ring. The NBO-series, and similarly the NBOMe-series (**Figure 12**), stem from the “2C”-series and

have methoxy groups at the 2- and 5- positions of the phenyl ring, a substitution on the 4- position of the phenyl ring, and a methoxy or other substitution at the 2- position of the *N*-benzyl ring [120]. The FLY-series and DRAGONFLY-series consists of tetrahydrobenzodifuran and benzodifuran located on the phenyl group where the only difference is the DRAGONFLY-series is fully substituted on this ring [121].

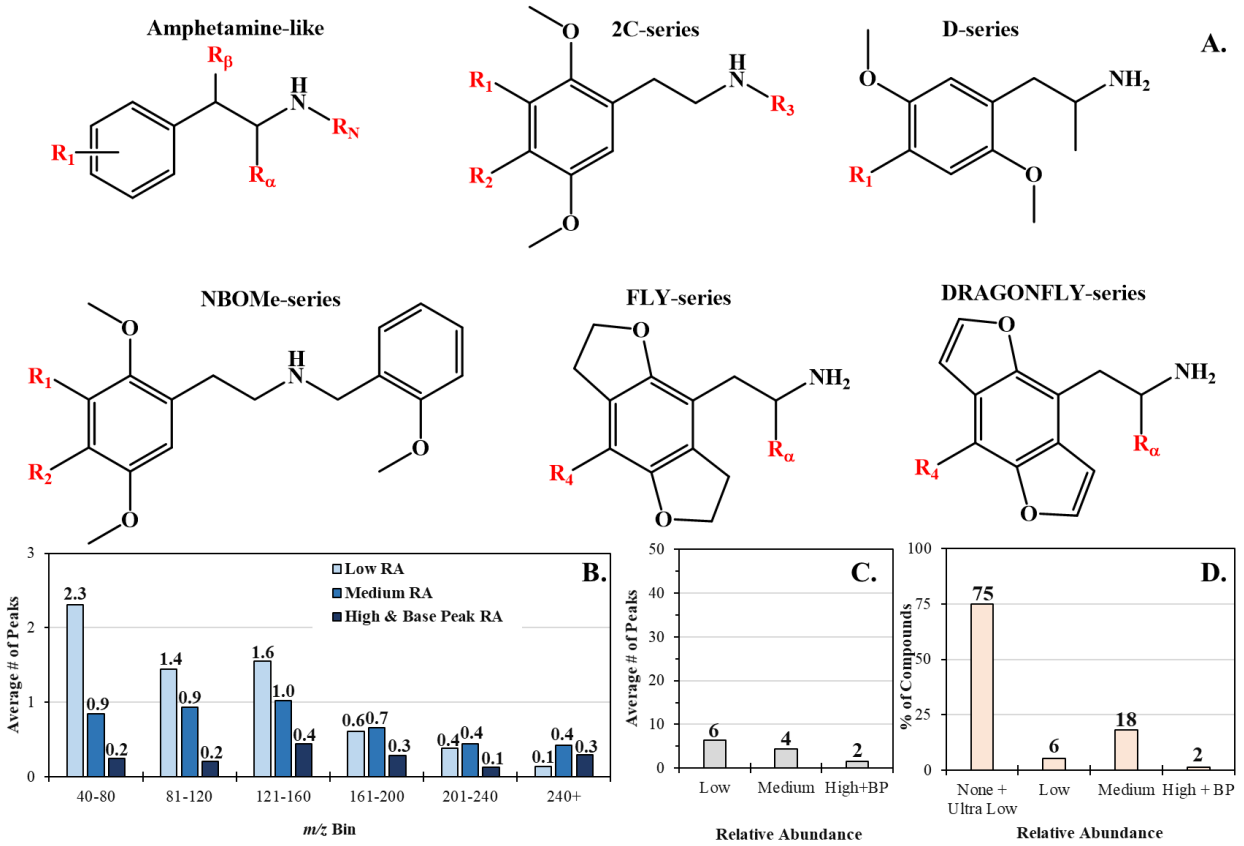

Figure 12: (A.) Common derivatives of the phenethylamine core structure [122]. (B.) Average distribution of *Low* (light blue), *Medium* (blue), and *High + Base Peak* (dark blue) ions across the *m/z* range, (C.) average number of peaks for each RA category (excluding *Ultra-Low*), and (D.) frequency of the presence of a molecular ion across the RA categories for the phenethylamines class (*n* = 127).

Compounds in this class that consist of amphetamine-like structures show similarities with the amphetamines class discussed above, dominated by a formation of ions at *m/z* 91 and *m/z* 44 (**Table 13**). Within the 2C class, there appear to be no common peaks. However, there are neutral losses of 15 Da, explained by the loss of the amino group. The D-series has very simplistic mass spectra with the primary base peak of *m/z* 44 followed by *Medium* peaks [123].

Table 13: Most frequently observed ions, neutral losses, and the total percentage of these values found in the phenethylamines class (*n* = 127). The neutral losses represent those from *Base Peak*, *High*, and *Medium* RA ions, combined.

Base Peak RA	High RA	Medium RA	Neutral Loss

m/z	Count (%)	*m/z*	Count (%)	*m/z*	Count (%)	Da	Count (%)
121	24 (19)	150	5 (4)	91	45 (35)	29	28 (22)
245	12 (9)	146	4 (3)	77	28 (22)	44	26 (20)
259	12 (9)	91	3 (2)	146	19 (15)	28	22 (17)
44	11 (9)	164	3 (2)	150	17 (13)	30	21 (17)
84	8 (6)	183	3 (2)	246	14 (11)	43	15 (12)
58	6 (5)	44	2 (2)	260	14 (11)	149	15 (12)
72	3 (2)	138	2 (2)	189	13 (10)	58	14 (11)
86	3 (2)	151	2 (2)	56	12 (9)	72	13 (10)
167	3 (2)	165	2 (2)	110	12 (9)	86	12 (9)
91	2 (2)	167	2 (2)	96	11 (9)	60	10 (8)

The NBOMe-phenethylamines have distinct spectra with characteristic fragments of the tropylium cation (*m*/*z* 91), the methoxy-substituted tropylium ion (*m*/*z* 121 (*Base Peak*)), and the methoxy-substituted tropylium ion with a secondary amine chain (*m*/*z* 150) [115]. Despite substitutions on the aromatic ring in the NBOMe-phenethylamines, these three ions dominate the spectra and consequently can be considered characteristic ions for this subclass [115].

The merged database consists of four compounds within the FLY and DragonFLY categories – 2C-B-FLY, N-(2C-B-fly) fentanyl, N-(3C-B-fly) fentanyl, and Bromo-Dragon-FLY. The two fentanyl analogs exhibit similar mass spectral characteristics to the fentanyl fragmentation *m/z* 146, *m/z* 189, and *m/z* 245. For the 2C-B-FLY and Bromo-Dragon-FLY compounds, both show isotopic signals of Br and fragmentation of the amino group on the tail. No further inferences were made for these compounds due to lack of compounds representing this specific structure. Based on the merged database information and reported literature, potential diagnostic characteristics of phenethylamines include (i) spectra with a *Base Peak* and up to one additional *High* RA peak, (ii) spectra with a higher number of *Medium* and *Low* RA peaks than other stimulant subclasses, (iii) spectra dominated with peaks below *m/z* 160, and (iv) spectra with either no molecular ion or a molecular ion with *Medium* RA. Common neutral losses are 29 Da and 44 Da.

3.1.6.4. Arylcyclohexylamines (n=42)

The arylcyclohexylamine subclass consists of commonly observed compounds, such as phencyclidine (PCP) which is one of the top 25 reported compounds [6], as well as novel emerging compounds such as recently reported F-PCP, Cl-PCP, POXP, and PTHP. Compounds in this class consist of a core structure with substitutions occurring at the aromatic ring (R_1), at the cyclohexane ring (R_2) , and at the amine moiety (R_3 and R_4) (**Figure 13**).

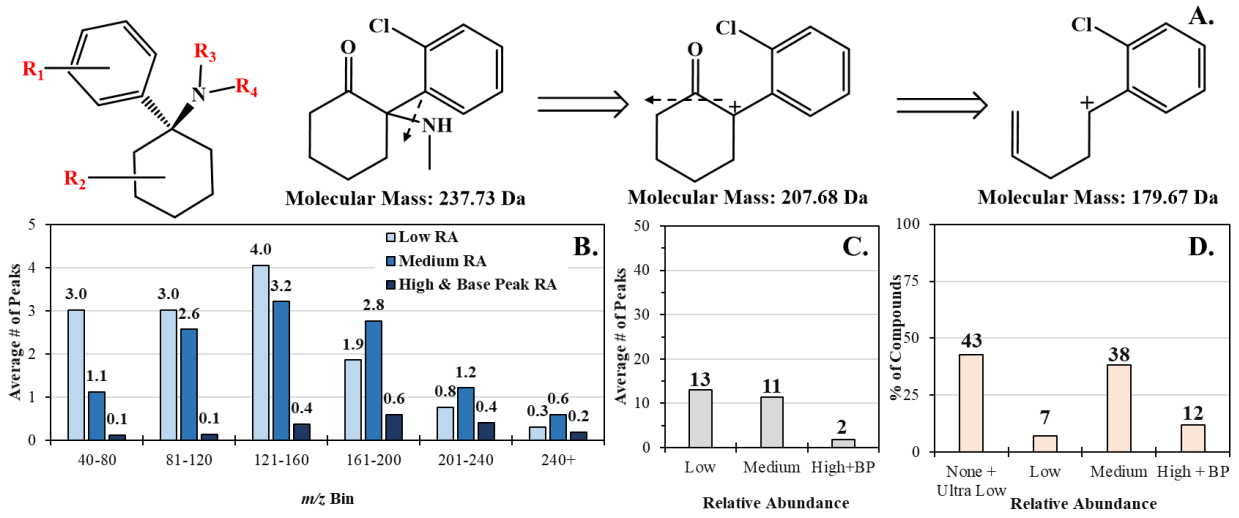

Figure 13: (A.) General core arylcyclohexylamines structure (left) and suggested fragmentation of ketamine (right) [124]. (B.) Average distribution of *Low* (light blue), *Medium* (blue), and *High + Base Peak* (dark blue) ions across the *m/z* range, (C.) average number of peaks for each RA category (excluding *Ultra-Low*), and (D.) frequency of the presence of a molecular ion across the RA categories for the arylcyclohexylamines class (n = 42).

Investigating the mass spectra of the 42 compounds in the merged database, there are no obvious trends within the *Base Peak* and *High* RA categories but there is commonality in the fragmentation pathways. For instance, compounds that are structurally similar to phencyclidine (PCP) exhibit neutral losses of 42/43 Da. Substances that have a neutral loss of 57 Da are indicative of a ketone substitution on the cyclohexane ring (**Figure 13**) which is found in ketamine-like compounds. Using the *NIST MS Interpreter* tool as a guide, other common neutral losses of 28 Da, 57 Da, and 85 Da are caused by various fragmentation across the cyclohexane ring.

Table 14: Most frequently observed ions, neutral losses, and the total percentage of these values found in the arylcyclohexylamines class (n = 42). The neutral losses represent those from *Base Peak*, *High*, and *Medium* RA ions, combined.

Base Peak RA		High RA		Medium RA		Neutral Loss	
m/z	**Count (%)**	***m/z***	**Count (%)**	***m/z***	**Count (%)**	**Da**	**Count (%)**
164	3 (7)	91	2 (5)	115	16 (38)	57	33 (79)
176	3 (7)	105	2 (5)	91	16 (38)	85	22 (52)
190	3 (7)	150	2 (5)	77	11 (26)	28	20 (48)
204	3 (7)	157	2 (5)	117	10 (24)	56	20 (48)
160	2 (5)	256	2 (5)	84	9 (21)	43	18 (43)
166	2 (5)			104	8 (19)	99	15 (36)
200	2 (5)			134	8 (19)	42	14 (33)
216	2 (5)			102	7 (17)	71	13 (31)
				166	7 (17)	113	13 (31)
				138	7 (17)	126	13 (31)

For the ions in the *Medium* RA category, *m/z* 91 and *m/z* 115 appear in 38 % of the compounds, suggesting fragmentation and formation of the phenyl ring with a variety of functional groups [80].

Based on the merged database information and reported literature, potential diagnostic characteristics of arylcyclohexylamines include (i) ions at *m/z* 91 and *m/z* 115, numerous *Low* and *Medium* RA ions spread across the mass range below *m/z* 200, and (iii) one to two *High* RA peaks in the *m/z* 120 to *m/z* 240 range. The presences, and RA, of a molecular ion is inconsistent. Common neutral losses for this class are 57 Da, 85 Da, 28 Da, 56 Da, and 43 Da.

3.1.6.5. Piperazines (n=28)

Piperazines are compounds often found at raves and other nightclubs and are sold as "ecstasy" pills or under names such as "Frenzy", "Bliss", "Charge", "Herbal ecstasy", "A2", "Legal X" and "Legal E" [125]. These compounds are not frequently encountered in casework, according to the NFLIS 2020 Annual Report [6], but do have a core structure that is amenable to substitution. The core structure of these substances is piperazine, and the types of compounds observed can be broken into three categories (**Figure 14A**) including benzylpiperazines (*i.e.*, N-benzylpiperazine (BZP)), phenylpiperazines (*i.e.*, 1-(3-chlorophenyl)piperazine (mCPP)), and thienylmethylpiperazines (*i.e.*, 1-[(5-Ethylthien-2-yl)methyl]piperazine) [125].

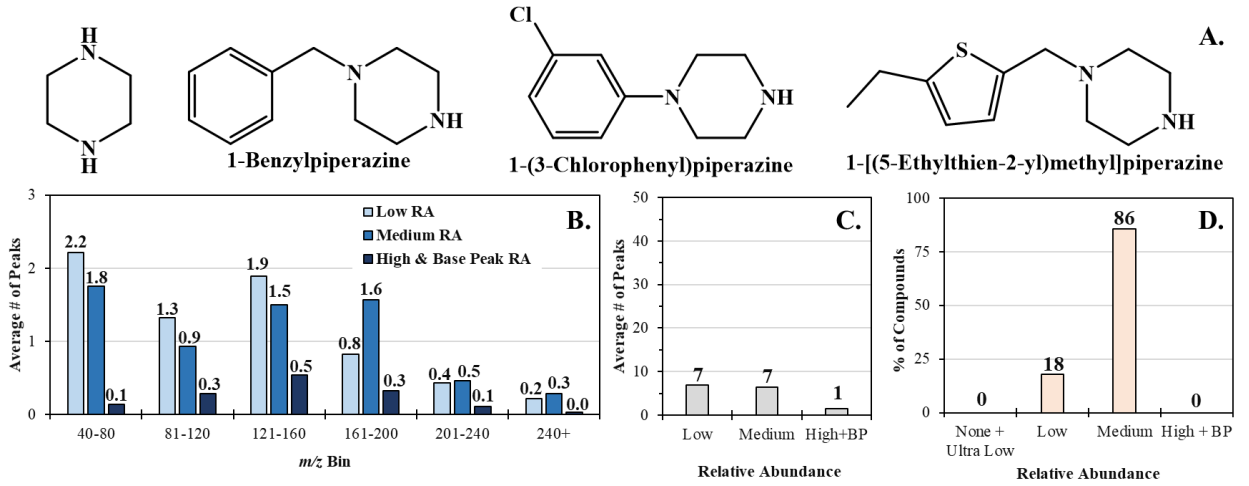

Figure 14: (A.) Core structure of piperazine ring and observed piperazine designer drugs [126,127]. (B.) Average distribution of *Low* (light blue), *Medium* (blue), and *High + Base Peak* (dark blue) ions across the *m/z* range, (C.) average number of peaks for each RA category (excluding *Ultra-Low*), and (D.) frequency of the presence of a molecular ion across the RA categories for the piperazines class (*n* = 28).

Investigating the mass spectra of the 28 compounds in the merged database, there are no obvious commonalities of the ions within the *Base Peak* and *High* RA categories, though fragmentation trends do exist. For instance, neutral losses of 42 Da, and 85 Da are common across the subclass (**Table 15**). Using the *NIST MS Interpreter* tool as a guide, each mass spectrum and their structures were combed for commonalities.

Table 15: Most frequently observed ions, neutral losses, and the total percentage of these values found in the piperazines class (n = 28). The neutral losses represent those from *Base Peak*, *High*, and *Medium* RA ions, combined.

Base Peak RA		**High RA**		**Medium RA**		**Neutral Loss**	
m/z	**Count (%)**	***m/z***	**Count (%)**	***m/z***	**Count (%)**	**Da**	**Count (%)**
91	4 (14)	56	2 (7)	56	18 (64)	42	22 (79)
188	4 (14)			85	6 (21)	85	20 (71)
138	3 (11)			230	5 (18)	57	14 (50)
105	2 (7)			65	4 (14)	58	14 (50)
135	2 (7)			172	4 (14)	40	7 (25)
150	2 (7)			122	4 (14)	56	7 (25)
154	2 (7)			156	4 (14)	41	5 (18)
172	2 (7)			173	4 (14)	91	4 (14)
				77	4 (14)	134	4 (14)
				91	4 (14)	84	3 (11)

Substances exhibiting a loss of 85 Da were found to be benzylpiperazines with substitutions on the aromatic ring. The traditional phenylpiperazine-like compounds, possessing substitutions on the aromatic ring, have *Base Peak* ions with neutral losses of 42 Da [128,129]. Neutral losses of 58 Da are also attributed to phenylpiperazine-like compounds where the nitrogen atoms are not connected to the phenyl ring [128,129]. There are few instances where a neutral loss 72 Da (*i.e.*, 1-(4-Methoxyphenyl)piperazine) is observed which indicates a phenylpiperazine-like with substitutions on both the aromatic and piperidine rings. Other instances occur with mass spectral differences of 91 Da where those structures share the core benzylpiperazine-like moiety but with bulkier side chains or different substitutions on the piperidine ring. Interestingly, these compounds always had a molecular ion present between 10 % and 50 % RA. Based on the merged database information and reported literature, potential diagnostic characteristics of piperazines include (i) presence of an ion at *m/z* 56 with *Medium* or *High* RA, (ii) only one peak of *High* RA along with several *Low* and *Medium* RA peaks below *m/z* 200, and (iii) presence of a molecular ion with *Low* or *Medium* RA. Common neutral losses include 42 Da, 85 Da, 57 Da, and 58 Da.

3.1.7. Hallucinogens

Hallucinogenic compounds are often found in plants and fungi [130] or are synthetic compounds based on these naturally occurring compounds [131]. Many of the phenethylamine substances, such as PCP and ketamine, can be categorized as both a stimulant and hallucinogen depending on dosage and target sites in the CNS [132–134]. Amongst the hallucinogens, the psychedelics are the most studied and reported substances and are typically comprised of phenethylamines and tryptamines [102,131,135,136].

3.1.7.1. Tryptamines (n=57)

Some well-known tryptamines like dimethyltryptamine (DMT), lysergic acid diethylamide (LSD), and psilocybin are either natural or semisynthetic products originating from various fungi or plants, and even animals [135,137]. These compounds are frequently reported in casework, with both LSD and psilocin being amongst the top 25 most frequently reported drugs in the NFLIS 2020 Annual Report [6]. NPS Discovery has also reported the observation of new, designer tryptamines, such as 4-acetoxy EPT, in recent months [7]. Tryptamines can be categorized into two subclasses based on structure composition, such as ergolines (synthesized from the ergot fungus) [138] and simple tryptamines [139]. .

The scaffolding of tryptamines varies between subclasses but are centered around the indole ring structure [138–141]. For simple tryptamines (**Figure 15**), the indole ring attaches to an amino group via a two-carbon sidechain (monoamine chain) and can have various substitutions at the nitrogen (R_{N1} and R_{N2}) and at the alpha carbon (R_{α}). Like the amphetamines class, the simple tryptamines readily dissociate at the α and β-carbon bond and have relatively simplistic mass spectra [142].

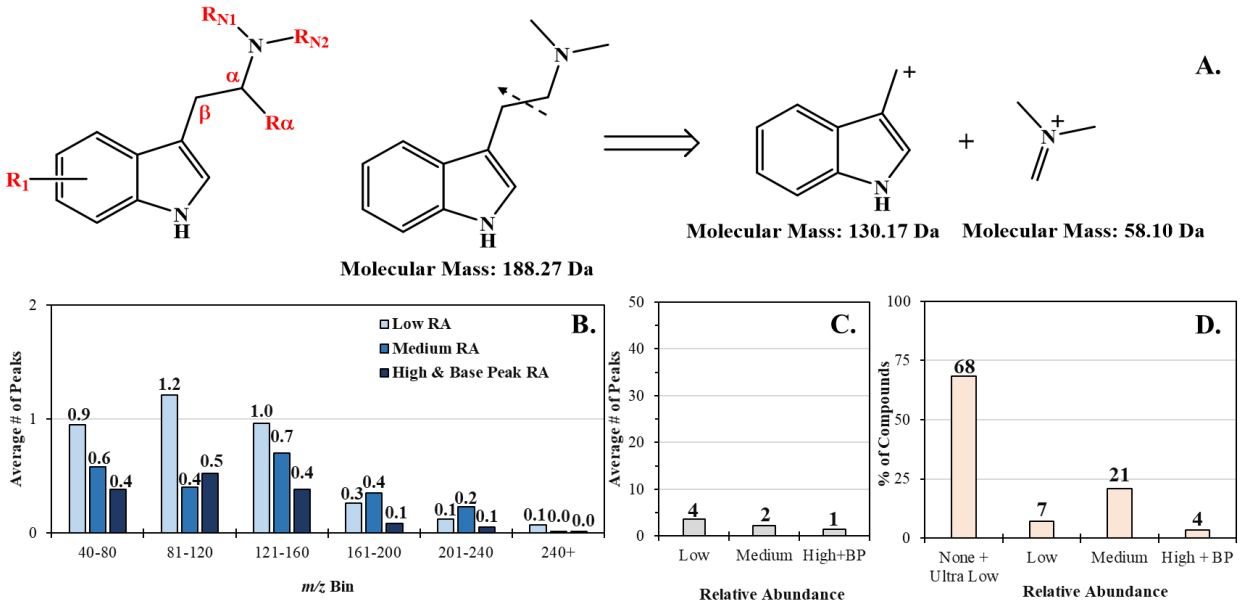

Figure 15: (A.) Core structure of tryptamines and proposed fragmentation for DMT [143]. (B.) Average distribution of Low (light blue), Medium (blue), and High + Base Peak (dark blue) ions across the m/z range, (C.) average number of peaks for each RA category (excluding *Ultra-Low*), and (D.) frequency of the presence of a molecular ion across the RA categories for the tryptamines class (n = 57).

For these substances, this fragmentation often involves the monoamine group and indole core. For the 57 simple tryptamine compounds, there are slight trends found amongst the *Base Peak* and

High RA categories (**Table 16**). Fragmentation of the α and β-carbon bond, resulting in amino groups with varying alkyl chains produces ions at *m/z* 58, *m/z* 72, *m/z* 86, *m/z* 100, *m/z* 114, and *m/z* 142. The *m/z* 84 ion is the product of the methyl-*N*-allyltryptamine (MALT) substances which has a double bond on the amino group.

Table 76: Most frequently observed ions, neutral losses, and the total percentage of these values found in the tryptamines class (*n* = 57). The neutral losses represent those from *Base Peak*, *High*, and *Medium* RA ions, combined.

Base Peak RA		**High RA**		**Medium RA**		**Neutral Loss**	
m/z	**Count (%)**	***m/z***	**Count (%)**	***m/z***	**Count (%)**	**Da**	**Count (%)**
114	12 (21)	44	5 (9)	146	9 (16)	160	17 (30)
58	11 (19)	130	5 (9)	160	9 (16)	130	12 (21)
86	11 (19)	58	2 (4)	44	8 (14)	188	12 (21)
72	3 (5)	131	2 (4)	72	8 (14)	146	10 (18)
100	3(5)			77	6 (11)	202	9 (16)
131	3 (5)			117	6 (11)	58	7 (12)
84	2 (4)			130	6 (11)	43	6 (11)
142	2 (4)			115	5 (9)	44	6 (11)
161	2 (4)			103	4 (7)	114	5 (9)
				143	4 (7)	29	4 (7)

The remaining fragment ions in the *Base Peak* and *High* RA categories (*m/z* 130, *m/z* 131, *m/z* 142, and *m/z* 161) correspond to a resulting α cleavage and an indole core structure with varying substitutions [142]. Based on the merged database information and reported literature, potential diagnostic characteristics of tryptamines include (i) an ion at *m/z* 58, *m/z* 72, *m/z* 86, *m/z* 100, and *m/z* 114, (ii) feature poor mass spectra exhibiting one or two *High* RA peak along with a higher number of *Medium* RA peaks, (iii) spectra with peaks below *m/z* 160, and (iv) either no or a *Medium* RA molecular ion. Neutral losses of 130 Da, 146 Da, 160 Da, and 188 Da are common and correspond to the remaining indole moiety with varying substitutions.

For the five LSD-like compounds (**Figure 16**), molecular ions are in the *High* RA category which is expected for these fused ring structures. Common ions reported within literature and the merged database investigation are *m/z* 181, *m/z* 207, and *m/z* 221 and cleaves across the fused ring.

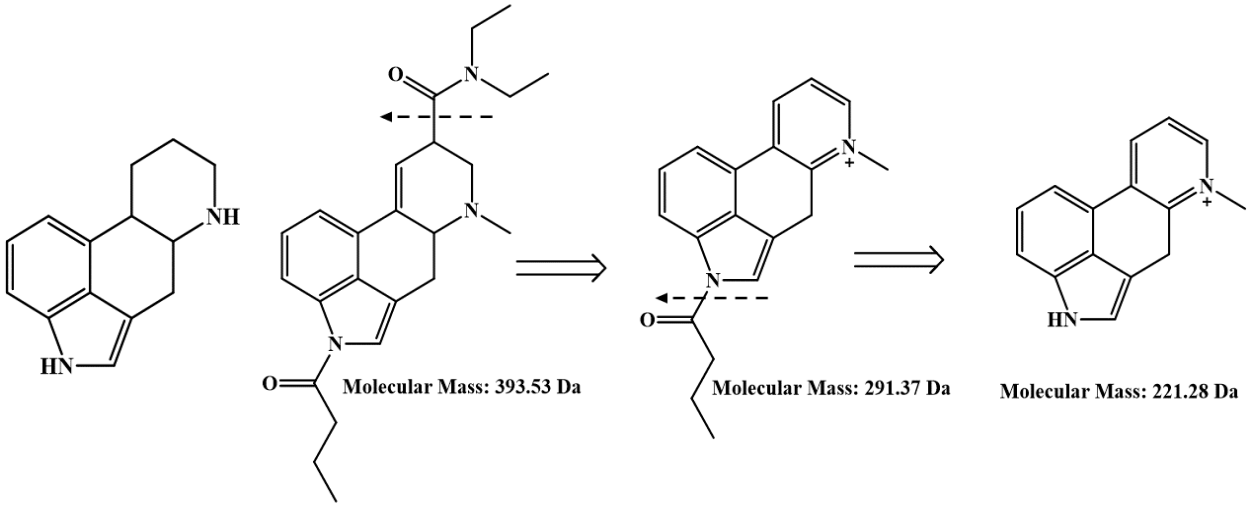

Figure 16: Core structure of tryptamines and proposed fragmentation for LSD [144].

Additionally, the neutral loss of 102 Da is common from the molecular ion to the next highest peak indicating an ergoline base structure with a methyl group [144,145]. These conclusions from the merged database investigation are conservative as there were only five LSD-type substance entries.

4. Conclusions

The influx of new/novel illicit psychoactive substances continues to strain limited resources and increase backlogs of forensic laboratories. For most drug chemists, GC-EI-MS remains the primary technique for identifying and characterizing NPSs. As discussed in this work, and highlighted in the *Supplemental Information*, there are mass spectral trends that can be used to help analysts classify unknown compounds. While this resource can help classify an unknown compound, definitive identification, especially when a standard is not available, will require the use of other analytical techniques or statistical approaches. Other analytical techniques that can provide additional information for structural elucidation include LC-MS/MS, H-NMR, spectroscopic methods, and DART-MS/MS [12,18,94,110,146–148]. An orthogonal approach is to leverage multivariate statistics or machine learning algorithms to identify important features contributing to compound characterization within mass spectra [11,15,43,149,150]. Use of this approach has been successful in differentiating illicit substances and positional isomers based upon mass spectra to explain the influence of slight structure modifications [40,64,79].

It should be noted that this work only discusses the mass spectral component of the GC-EI-MS and does not discuss chromatographic retention times, which can provide another critical component for unknown compound classification. Because of a lack of method standardization in

the field, no definitive statements can be made. However, individual laboratories can monitor retention times of known compounds and use them to better narrow down the potential class(es) of unknown compounds. Laboratories may also want to consider locked retention times or retention indices to allow for comparison of retention data across different methods. Ultimately, the interest of the forensic community to increase and understand common trends in drug analysis is crucial as it can potentially lead to quicker characterizations and decrease backlogs.

Author Contributions

The manuscript was written through the contributions of all authors. All authors have given approval to the final version of the manuscript.

CRediT authorship contribution statement

William Feeney (ORCID – 0000-0001-7218-3449)**:** Conceptualization, Formal analysis, Writing - original draft.
Arun S. Moorthy (ORCID – 0000-0002-5988-1389)**:** Formal analysis, Troubleshooting, Writing - review & editing.
Edward Sisco (ORCID – 0000-0003-0252-1910)**:** Supervision, Formal analysis, Writing - review & editing

Declaration of Competing Interest

The authors declare that they have no known competing financial interests or personal relationships that could have appeared to influence the work reported in this paper.

Disclaimer

Certain commercial products are identified in order to adequately specify the procedure; this does not imply endorsement or recommendation by NIST, nor does it imply that such products are necessarily the best available for the purpose.

Acknowledgments

A special thanks goes to Joe Rundle from Cayman Chemical for providing the compound class information to use in this investigation.

5. References

[1] D. Ciccarone, The rise of illicit fentanyls, stimulants and the fourth wave of the opioid overdose crisis, Current Opinion in Psychiatry. 34 (2021) 344–350. https://doi.org/10.1097/YCO.0000000000000717.
[2] V. Lukić, R. Micić, B. Arsić, B. Nedović, Ž. Radosavljević, Overview of the major classes of new psychoactive substances, psychoactive effects, analytical determination and

conformational analysis of selected illegal drugs, Open Chemistry. 19 (2021) 60–106. https://doi.org/10.1515/chem-2021-0196.
[3] S. Strano Rossi, S. Odoardi, A. Gregori, G. Peluso, L. Ripani, G. Ortar, G. Serpelloni, F.S. Romolo, An analytical approach to the forensic identification of different classes of new psychoactive substances (NPSs) in seized materials: Analytical approach for the identification of NPSs in seizures, Rapid Commun. Mass Spectrom. 28 (2014) 1904–1916. https://doi.org/10.1002/rcm.6969.
[4] V. Coopman, P. Blanckaert, G. Van Parys, S. Van Calenbergh, J. Cordonnier, A case of acute intoxication due to combined use of fentanyl and 3,4-dichloro-N-[2-(dimethylamino)cyclohexyl]-N-methylbenzamide (U-47700), Forensic Science International. 266 (2016) 68–72. https://doi.org/10.1016/j.forsciint.2016.05.001.
[5] E. Gerace, A. Salomone, C. Luciano, D. Di Corcia, M. Vincenti, First Case in Italy of Fatal Intoxication Involving the New Opioid U-47700, Frontiers in Pharmacology. 9 (2018). https://www.frontiersin.org/article/10.3389/fphar.2018.00747 (accessed March 2, 2022).
[6] U.S. Drug Enforcement Administration, Diversion Control Division, National Forensic Laboratory Information System: 2020 Annual Report, (2020).
[7] Center for Forensic Science Research and Education (CFSRE), 2021 Year in Review, NPS Discovery. (2021). https://www.npsdiscovery.org/.
[8] A. Urbas, T. Schoenberger, C. Corbett, K. Lippa, F. Rudolphi, W. Robien, NPS Data Hub: A web-based community driven analytical data repository for new psychoactive substances, Forensic Chemistry. 9 (2018) 76–81. https://doi.org/10.1016/j.forc.2018.05.003.
[9] M. von Cüpper, P.W. Dalsgaard, K. Linnet, Identification of New Psychoactive Substances in Seized material Using UHPLC–QTOF-MS and An Online Mass Spectral Database, Journal of Analytical Toxicology. 44 (2020) 1047–1051. https://doi.org/10.1093/jat/bkaa028.
[10] D.M. Walentiny, L.T. Moisa, P.M. Beardsley, Oxycodone-like discriminative stimulus effects of fentanyl-related emerging drugs of abuse in mice, Neuropharmacology. 150 (2019) 210–216. https://doi.org/10.1016/j.neuropharm.2019.02.007.
[11] A.S. Moorthy, A.J. Kearsley, W.G. Mallard, W.E. Wallace, Mass spectral similarity mapping applied to fentanyl analogs, Forensic Chemistry. 19 (2020) 100237. https://doi.org/10.1016/j.forc.2020.100237.
[12] E. Sisco, J. Verkouteren, J. Staymates, J. Lawrence, Rapid detection of fentanyl, fentanyl analogues, and opioids for on-site or laboratory based drug seizure screening using thermal desorption DART-MS and ion mobility spectrometry, Forensic Chemistry. 4 (2017) 108–115. https://doi.org/10.1016/j.forc.2017.04.001.
[13] C. Soussan, M. Andersson, A. Kjellgren, The diverse reasons for using Novel Psychoactive Substances - A qualitative study of the users' own perspectives, International Journal of Drug Policy. 52 (2018) 71–78. https://doi.org/10.1016/j.drugpo.2017.11.003.
[14] M.M. Vandeputte, K. Van Uytfanghe, N.K. Layle, D.M. St. Germaine, D.M. Iula, C.P. Stove, Synthesis, Chemical Characterization, and μ-Opioid Receptor Activity Assessment of the Emerging Group of "Nitazene" 2-Benzylbenzimidazole Synthetic Opioids, ACS Chem. Neurosci. 12 (2021) 1241–1251. https://doi.org/10.1021/acschemneuro.1c00064.
[15] P. Koshute, N. Hagan, N.J. Jameson, Machine learning model for detecting fentanyl analogs from mass spectra, Forensic Chemistry. 27 (2022) 100379. https://doi.org/10.1016/j.forc.2021.100379.
[16] M. Cauchi, C.M. Weber, B.J. Bolt, P.B. Spratt, C. Bessant, D.C. Turner, C.M. Willis, L.E. Britton, C. Turner, G. Morgan, Evaluation of gas chromatography mass spectrometry and

pattern recognition for the identification of bladder cancer from urine headspace, Anal. Methods. 8 (2016) 4037–4046. https://doi.org/10.1039/C6AY00400H.
[17] K. Kelly, S. Bell, Evaluation of the reproducibility and repeatability of GCMS retention indices and mass spectra of novel psychoactive substances, Forensic Chemistry. 7 (2018) 10–18. https://doi.org/10.1016/j.forc.2017.11.002.
[18] E.L. Robinson, E. Sisco, Detection of Brodifacoum and other Rodenticides in Drug Mixtures using Thermal Desorption Direct Analysis in Real Time Mass Spectrometry (TD-DART-MS), Journal of Forensic Sciences. 64 (2019) 1026–1033. https://doi.org/10.1111/1556-4029.13978.
[19] SWGDRUG, Scientific Working Group for the Analysis of Seized Drugs (Recommendations), (2019). www.swgdrug.org.
[20] W.E. Wallace, W. Ji, D.V. Tchekhovskoi, K.W. Phinney, S.E. Stein, Mass Spectral Library Quality Assurance by Inter-Library Comparison, J Am Soc Mass Spectrom. 28 (2017) 733–738. https://doi.org/10.1007/s13361-016-1589-4.
[21] J.H. Gross, Mass Spectrometry, Springer International Publishing, Cham, 2017. https://doi.org/10.1007/978-3-319-54398-7.
[22] R. Ekman, ed., Mass spectrometry: instrumentation, interpretation, and applications, John Wiley & Sons, Hoboken, N.J, 2009.
[23] United Nations Office of Drugs and Crime, Recommended methods for the identification and analysis of Barbiturates and Benzodiazepines under International Control, (2012) 78.
[24] M. Butler, G.M. Cabrera, A mass spectrometry-based method for differentiation of positional isomers of monosubstituted pyrazine N-oxides using metal ion complexes, Journal of Mass Spectrometry. 50 (2015) 136–144. https://doi.org/10.1002/jms.3506.
[25] Barbiturates, in: Meyler's Side Effects of Drugs, Elsevier, 2016: pp. 819–826. https://doi.org/10.1016/B978-0-444-53717-1.00033-0.
[26] J.P. Buchweitz, M. Johnson, J.L. Jones, A.F. Lehner, Development of a Quantitative Gas Chromatography–Tandem Mass Spectrometry Method for the Determination of Pentobarbital in Dog Food, J. Agric. Food Chem. 66 (2018) 11166–11169. https://doi.org/10.1021/acs.jafc.8b04178.
[27] H. Zhao, L. Wang, Y. Qiu, Z. Zhou, X. Li, W. Zhong, Simultaneous determination of three residual barbiturates in pork using accelerated solvent extraction and gas chromatography–mass spectrometry, Journal of Chromatography B. 840 (2006) 139–145. https://doi.org/10.1016/j.jchromb.2006.05.002.
[28] H. Tian, X. Zhou, C. Chen, Y. He, H. Yu, X. Zheng, Simultaneous Determination of Phenobarbital, Pentobarbital, Amobarbital and Secobarbital in Raw Milk via Liquid Chromatography with Electron Spray Ionization Tandem Mass Spectrometry, Food Science of Animal Resources. 37 (2017) 847–854. https://doi.org/10.5851/kosfa.2017.37.6.847.
[29] M. Peschka, J.P. Eubeler, T.P. Knepper, Occurrence and Fate of Barbiturates in the Aquatic Environment, Environ. Sci. Technol. 40 (2006) 7200–7206. https://doi.org/10.1021/es052567r.
[30] P. Szatkowska, M. Koba, P. Kośliński, J. Wandas, T. Bączek, Analytical methods for determination of benzodiazepines. A short review, Open Chemistry. 12 (2014) 994–1007. https://doi.org/10.2478/s11532-014-0551-1.
[31] R.-Y. Hsu, S.-A. Chan, S.-L. Lin, T.-Y. Lin, W.-L. Chu, M.-R. Fuh, Direct quantitative analysis of benzodiazepines, metabolites, and analogs in diluted human urine by rapid

resolution liquid chromatography–tandem mass spectrometry, Journal of Food and Drug Analysis. 21 (2013) 376–383. https://doi.org/10.1016/j.jfda.2013.08.005.
[32] T.J.P. Smyth, V. Rodríguez Robledo, W.F. Smyth, Characterisation of oxazepam degradation products by high-performance liquid chromatography/electrospray ionisation mass spectrometry and electrospray ionisation quadrupole time-of-flight tandem mass spectrometry, Rapid Commun Mass Spectrom. 24 (2010) 651–658. https://doi.org/10.1002/rcm.4433.
[33] M. Rida, H.E. Meslouhi, N.-E. Es-Safi, E.M. Essassi, J. Banoub, Gas-phase fragmentation study of novel synthetic 1,5-benzodiazepine derivatives using electrospray ionization tandem mass spectrometry, Rapid Communications in Mass Spectrometry. 22 (2008) 2253–2268. https://doi.org/10.1002/rcm.3612.
[34] W. Sadee, Mechanism of metabolic 3-hydroxylation of benzodiazepines. Fragmentation pattern of 1,4-benzodiazepin-2-ones under electron impact, J. Med. Chem. 13 (1970) 475–479. https://doi.org/10.1021/jm00297a032.
[35] A.C. Gelebe, P.T. Kaye, Benzodiazepine Analogues. Part 20. Mass Spectrometric Analysis of Benzoxathiepine Derivatives, J. Chem. Res. (S). (1999) 584–585. https://doi.org/10.1039/A902499I.
[36] S. Watanabe, S. Vikingsson, A. Åstrand, V. Auwärter, H. Gréen, R. Kronstrand, Metabolism of the benzodiazepines norflurazepam, flurazepam, fludiazepam and cinolazepam by human hepatocytes using high-resolution mass spectrometry and distinguishing their intake in authentic urine samples, Forensic Toxicol. 38 (2020) 79–94. https://doi.org/10.1007/s11419-019-00488-9.
[37] A.G. Fragkaki, Y.S. Angelis, A. Tsantili-Kakoulidou, M. Koupparis, C. Georgakopoulos, Statistical analysis of fragmentation patterns of electron ionization mass spectra of enolized-trimethylsilylated anabolic androgenic steroids, International Journal of Mass Spectrometry. 285 (2009) 58–69. https://doi.org/10.1016/j.ijms.2009.04.008.
[38] A.G. Fragkaki, Y.S. Angelis, M. Koupparis, A. Tsantili-Kakoulidou, G. Kokotos, C. Georgakopoulos, Structural characteristics of anabolic androgenic steroids contributing to binding to the androgen receptor and to their anabolic and androgenic activities, Steroids. 74 (2009) 172–197. https://doi.org/10.1016/j.steroids.2008.10.016.
[39] A.G. Fragkaki, Y.S. Angelis, A. Tsantili-Kakoulidou, M. Koupparis, C. Georgakopoulos, Schemes of metabolic patterns of anabolic androgenic steroids for the estimation of metabolites of designer steroids in human urine, The Journal of Steroid Biochemistry and Molecular Biology. 115 (2009) 44–61. https://doi.org/10.1016/j.jsbmb.2009.02.016.
[40] G. Lee, E. Park, H. Chung, Y. Jeanvoine, K. Song, R. Spezia, Gas phase fragmentation mechanisms of protonated testosterone as revealed by chemical dynamics simulations, International Journal of Mass Spectrometry. 407 (2016) 40–50. https://doi.org/10.1016/j.ijms.2016.07.001.
[41] T.F. Kalhorn, S.T. Page, W.N. Howald, E.A. Mostaghel, P.S. Nelson, Analysis of testosterone and dihydrotestosterone from biological fluids as the oxime derivatives using high-performance liquid chromatography/tandem mass spectrometry, Rapid Commun. Mass Spectrom. 21 (2007) 3200–3206. https://doi.org/10.1002/rcm.3205.
[42] M. Thevis, W. Schänzer, Mass spectrometric analysis of androstan-17β-ol-3-one and androstadiene-17β-ol-3-one isomers, J. Am. Soc. Mass Spectrom. 16 (2005) 1660–1669. https://doi.org/10.1016/j.jasms.2005.06.007.

[43] M. Thevis, A.A. Makarov, S. Horning, W. Schänzer, Mass spectrometry of stanozolol and its analogues using electrospray ionization and collision-induced dissociation with quadrupole-linear ion trap and linear ion trap-orbitrap hybrid mass analyzers, Rapid Communications in Mass Spectrometry. 19 (2005) 3369–3378. https://doi.org/10.1002/rcm.2204.
[44] N.S. Rannulu, R.B. Cole, Novel Fragmentation Pathways of Anionic Adducts of Steroids Formed by Electrospray Anion Attachment Involving Regioselective Attachment, Regiospecific Decompositions, Charge-Induced Pathways, and Ion–Dipole Complex Intermediates, J. Am. Soc. Mass Spectrom. 23 (2012) 1558–1568. https://doi.org/10.1007/s13361-012-0422-y.
[45] M. Yamada, S. Aramaki, T. Okayasu, T. Hosoe, M. Kurosawa, I. Kijima-Suda, K. Saito, H. Nakazawa, Identification and quantification of metabolites common to 17α-methyltestosterone and mestanolone in horse urine, Journal of Pharmaceutical and Biomedical Analysis. 45 (2007) 125–133. https://doi.org/10.1016/j.jpba.2007.06.020.
[46] T.M. Williams, A.J. Kind, E. Houghton, D.W. Hill, Electrospray collision-induced dissociation of testosterone and testosterone hydroxy analogs, Journal of Mass Spectrometry. 34 (1999) 206–216. https://doi.org/10.1002/(SICI)1096-9888(199903)34:3<206::AID-JMS785>3.0.CO;2-1.
[47] F. Guan, L.R. Soma, Y. Luo, C.E. Uboh, S. Peterman, Collision-induced dissociation pathways of anabolic steroids by electrospray ionization tandem mass spectrometry, J. Am. Soc. Mass Spectrom. 17 (2006) 477–489. https://doi.org/10.1016/j.jasms.2005.11.021.
[48] M. Thevis, S. Beuck, S. Höppner, A. Thomas, J. Held, M. Schäfer, J. Oomens, W. Schänzer, Structure Elucidation of the Diagnostic Product Ion at m/z 97 Derived from Androst-4-en-3-One-Based Steroids by ESI-CID and IRMPD Spectroscopy, J. Am. Soc. Mass Spectrom. 23 (2012) 537–546. https://doi.org/10.1007/s13361-011-0308-4.
[49] M.K. Parr, J. Zapp, M. Becker, G. Opfermann, U. Bartz, W. Schänzer, Steroidal isomers with uniform mass spectra of their per-TMS derivatives: Synthesis of 17-hydroxyandrostan-3-ones, androst-1-, and -4-ene-3,17-diols, Steroids. 72 (2007) 545–551. https://doi.org/10.1016/j.steroids.2007.03.006.
[50] J. Chilakapati, F.F. Farris, Cannabinoids, in: P. Wexler (Ed.), Encyclopedia of Toxicology (Third Edition), Academic Press, Oxford, 2014: pp. 649–654. https://doi.org/10.1016/B978-0-12-386454-3.00267-0.
[51] K.A. Seely, J. Lapoint, J.H. Moran, L. Fattore, Spice drugs are more than harmless herbal blends: A review of the pharmacology and toxicology of synthetic cannabinoids, Progress in Neuro-Psychopharmacology and Biological Psychiatry. 39 (2012) 234–243. https://doi.org/10.1016/j.pnpbp.2012.04.017.
[52] A.C. Howlett, C.S. Breivogel, S.R. Childers, S.A. Deadwyler, R.E. Hampson, L.J. Porrino, Cannabinoid physiology and pharmacology: 30 years of progress, Neuropharmacology. 47 (2004) 345–358. https://doi.org/10.1016/j.neuropharm.2004.07.030.
[53] I. Vardakou, C. Pistos, Ch. Spiliopoulou, Spice drugs as a new trend: Mode of action, identification and legislation, Toxicology Letters. 197 (2010) 157–162. https://doi.org/10.1016/j.toxlet.2010.06.002.
[54] G. dos R.R. Franco, S. Smid, C. Viegas, Phytocannabinoids: General Aspects and Pharmacological Potential in Neurodegenerative Diseases, Curr Neuropharmacol. 19 (2021) 449–464. https://doi.org/10.2174/1570159X18666200720172624.

[55] G. Stefkov, I. Cvetkovikj Karanfilova, V. Stoilkovska Gjorgievska, A. Trajkovska, N. Geskovski, M. Karapandzova, S. Kulevanova, Analytical Techniques for Phytocannabinoid Profiling of Cannabis and Cannabis-Based Products—A Comprehensive Review, Molecules. 27 (2022) 975. https://doi.org/10.3390/molecules27030975.
[56] A. Leghissa, Z.L. Hildenbrand, F.W. Foss, K.A. Schug, Determination of cannabinoids from a surrogate hops matrix using multiple reaction monitoring gas chromatography with triple quadrupole mass spectrometry, Journal of Separation Science. 41 (2018) 459–468. https://doi.org/10.1002/jssc.201700946.
[57] M.M. Delgado-Povedano, C. Sánchez-Carnerero Callado, F. Priego-Capote, C. Ferreiro-Vera, Untargeted characterization of extracts from Cannabis sativa L. cultivars by gas and liquid chromatography coupled to mass spectrometry in high resolution mode, Talanta. 208 (2020) 120384. https://doi.org/10.1016/j.talanta.2019.120384.
[58] J.V. Johnson, A. Christensen, D. Morgan, K.B. Basso, Chapter Eight - Gas chromatography/electron ionization mass spectrometry (GC/EI-MS) for the characterization of phytocannabinoids in Cannabis sativa, in: I. Ferrer, E.M. Thurman (Eds.), Comprehensive Analytical Chemistry, Elsevier, 2020: pp. 235–274. https://doi.org/10.1016/bs.coac.2020.05.003.
[59] J. Jung, M.R. Meyer, H.H. Maurer, C. Neusüß, W. Weinmann, V. Auwärter, Studies on the metabolism of the Δ9-tetrahydrocannabinol precursor Δ9-tetrahydrocannabinolic acid A (Δ9-THCA-A) in rat using LC-MS/MS, LC-QTOF MS and GC-MS techniques, Journal of Mass Spectrometry. 44 (2009) 1423–1433. https://doi.org/10.1002/jms.1624.
[60] K. de C. Mariotti, M.C.A. Marcelo, R.S. Ortiz, B.T. Borille, M. dos Reis, M.S. Fett, M.F. Ferrão, R.P. Limberger, Seized cannabis seeds cultivated in greenhouse: A chemical study by gas chromatography–mass spectrometry and chemometric analysis, Science & Justice. 56 (2016) 35–41. https://doi.org/10.1016/j.scijus.2015.09.002.
[61] J.V. Johnson, A. Christensen, D. Morgan, K.B. Basso, Gas chromatography/electron ionization mass spectrometry (GC/EI-MS) for the characterization of phytocannabinoids in Cannabis sativa, in: Comprehensive Analytical Chemistry, Elsevier, 2020: pp. 235–274. https://doi.org/10.1016/bs.coac.2020.05.003.
[62] E.W. Gunderson, H.M. Haughey, N. Ait-Daoud, A.S. Joshi, C.L. Hart, "Spice" and "K2" Herbal Highs: A Case Series and Systematic Review of the Clinical Effects and Biopsychosocial Implications of Synthetic Cannabinoid Use in Humans, The American Journal on Addictions. 21 (2012) 320–326. https://doi.org/10.1111/j.1521-0391.2012.00240.x.
[63] V. Abbate, M. Schwenk, B.C. Presley, N. Uchiyama, The ongoing challenge of novel psychoactive drugs of abuse. Part I. Synthetic cannabinoids (IUPAC Technical Report), Pure and Applied Chemistry. 90 (2018) 1255–1282. https://doi.org/10.1515/pac-2017-0605.
[64] D.N. Harris, S. Hokanson, V. Miller, G.P. Jackson, Fragmentation differences in the EI spectra of three synthetic cannabinoid positional isomers: JWH-250, JWH-302, and JWH-201, International Journal of Mass Spectrometry. 368 (2014) 23–29. https://doi.org/10.1016/j.ijms.2014.05.005.
[65] V. Angerer, P. Bisel, B. Moosmann, F. Westphal, V. Auwärter, Separation and structural characterization of the new synthetic cannabinoid JWH-018 cyclohexyl methyl derivative "NE-CHMIMO" using flash chromatography, GC-MS, IR and NMR spectroscopy, Forensic Science International. 266 (2016) e93–e98. https://doi.org/10.1016/j.forsciint.2016.05.031.

[66] V. Shevyrin, V. Melkozerov, A. Nevero, O. Eltsov, Y. Shafran, Y. Morzherin, A.T. Lebedev, Identification and analytical characteristics of synthetic cannabinoids with an indazole-3-carboxamide structure bearing a N-1-methoxycarbonylalkyl group, Anal Bioanal Chem. 407 (2015) 6301–6315. https://doi.org/10.1007/s00216-015-8612-7.
[67] K. Sekuła, D. Zuba, K. Lorek, Analysis of Fragmentation Pathways of New-Type Synthetic Cannabinoids Using Electrospray Ionization, J. Am. Soc. Mass Spectrom. 29 (2018) 1941–1950. https://doi.org/10.1007/s13361-018-2008-9.
[68] J. Carlier, X. Diao, C. Sempio, M.A. Huestis, Identification of New Synthetic Cannabinoid ADB-CHMINACA (MAB-CHMINACA) Metabolites in Human Hepatocytes, AAPS J. 19 (2017) 568–577. https://doi.org/10.1208/s12248-016-0037-5.
[69] A. Wurita, K. Hasegawa, K. Minakata, K. Gonmori, H. Nozawa, I. Yamagishi, K. Watanabe, O. Suzuki, Identification and quantitation of 5-fluoro-ADB-PINACA and MAB-CHMINACA in dubious herbal products, Forensic Toxicol. 33 (2015) 213–220. https://doi.org/10.1007/s11419-015-0264-y.
[70] K. Hasegawa, A. Wurita, K. Minakata, K. Gonmori, H. Nozawa, I. Yamagishi, K. Watanabe, O. Suzuki, Postmortem distribution of MAB-CHMINACA in body fluids and solid tissues of a human cadaver, Forensic Toxicol. 33 (2015) 380–387. https://doi.org/10.1007/s11419-015-0272-y.
[71] K.L. Samano, J.L. Poklis, A.H. Lichtman, A. Poklis, Development of a High-Performance Liquid Chromatography–Tandem Mass Spectrometry Method for the Identification and Quantification of CP-47,497, CP-47,497-C8 and JWH-250 in Mouse Brain, Journal of Analytical Toxicology. 38 (2014) 307–314. https://doi.org/10.1093/jat/bku043.
[72] A. Namera, M. Kawamura, A. Nakamoto, T. Saito, M. Nagao, Comprehensive review of the detection methods for synthetic cannabinoids and cathinones, Forensic Toxicol. 33 (2015) 175–194. https://doi.org/10.1007/s11419-015-0270-0.
[73] E. Smolianitski-Fabian, E. Cohen, M. Dronova, A. Voloshenko-Rossin, O. Lev, Discrimination between closely related synthetic cannabinoids by GC-Cold-EI-MS, Drug Test Anal. 10 (2018) 474–487. https://doi.org/10.1002/dta.2247.
[74] M.P. Dybowski, P. Holowinski, R. Typek, A.L. Dawidowicz, Comprehensive analytical and structural characteristics of methyl 3,3-dimethyl-2-(1-(pent-4-en-1-yl)-1H-indazole-3-carboxamido)butanoate (MDMB-4en-PINACA), Forensic Toxicol. 39 (2021) 481–492. https://doi.org/10.1007/s11419-021-00573-y.
[75] V. Lukic, R. Micic, B. Arsic, M. Mitic, M. Jovanovic, A. Pavlovic, Identification of synthetic cannabinoid methyl 2-{[1-(cyclohexylmethyl)-1H-indol-3-yl] formamido}-3-methylbutanoate using modern mass spectrometry and nuclear magnetic resonance techniques, Open Chemistry. 19 (2021) 1250–1264. https://doi.org/10.1515/chem-2021-0113.
[76] M.G. Carlin, J.R. Dean, J.M. Ames, Opium Alkaloids in Harvested and Thermally Processed Poppy Seeds, Frontiers in Chemistry. 8 (2020). https://www.frontiersin.org/article/10.3389/fchem.2020.00737.
[77] J. Klingberg, A. Cawley, R. Shimmon, S. Fu, Collision-Induced Dissociation Studies of Synthetic Opioids for Non-targeted Analysis, Frontiers in Chemistry. 7 (2019). https://www.frontiersin.org/article/10.3389/fchem.2019.00331 (accessed March 1, 2022).
[78] S.A. Shetge, M.P. Dzakovich, J.L. Cooperstone, D. Kleinmeier, B.W. Redan, Concentrations of the Opium Alkaloids Morphine, Codeine, and Thebaine in Poppy Seeds are Reduced after Thermal and Washing Treatments but are Not Affected when Incorporated in a Model Baked

Product, J. Agric. Food Chem. 68 (2020) 5241–5248. https://doi.org/10.1021/acs.jafc.0c01681.
[79] Z. Zhang, B. Yan, K. Liu, T. Bo, Y. Liao, H. Liu, Fragmentation pathways of heroin-related alkaloids revealed by ion trap and quadrupole time-of-flight tandem mass spectrometry, Rapid Communications in Mass Spectrometry. 22 (2008) 2851–2862. https://doi.org/10.1002/rcm.3686.
[80] L. Bijlsma, J.V. Sancho, F. Hernández, W.M.A. Niessen, Fragmentation pathways of drugs of abuse and their metabolites based on QTOF MS/MS and MS(E) accurate-mass spectra, J Mass Spectrom. 46 (2011) 865–875. https://doi.org/10.1002/jms.1963.
[81] E.J. Fox, S. Twigger, K.R. Allen, Criteria for opiate identification using liquid chromatography linked to tandem mass spectrometry: problems in routine practice, Ann Clin Biochem. 46 (2009) 50–57. https://doi.org/10.1258/acb.2008.008104.
[82] N. Gilbert, R.E. Mewis, O.B. Sutcliffe, Classification of fentanyl analogues through principal component analysis (PCA) and hierarchical clustering of GC–MS data, Forensic Chemistry. 21 (2020) 100287. https://doi.org/10.1016/j.forc.2020.100287.
[83] J.T. Davidson, Z.J. Sasiene, G.P. Jackson, The characterization of isobaric product ions of fentanyl using multi-stage mass spectrometry, high-resolution mass spectrometry and isotopic labeling, Drug Test Anal. 12 (2020) 496–503. https://doi.org/10.1002/dta.2758.
[84] H. Ohta, S. Suzuki, K. Ogasawara, Studies on Fentanyl and Related Compounds IV. Chromatographic and Spectrometric Discrimination of Fentanyl and its Derivatives, Journal of Analytical Toxicology. 23 (1999) 280–285. https://doi.org/10.1093/jat/23.4.280.
[85] T. Breindahl, A. Kimergård, M.F. Andreasen, D.S. Pedersen, Identification of a new psychoactive substance in seized material: the synthetic opioid N-phenyl-N-[1-(2-phenethyl)piperidin-4-yl]prop-2-enamide (Acrylfentanyl), Drug Test Anal. 9 (2017) 415–422. https://doi.org/10.1002/dta.2046.
[86] H.G. Pierzynski, L. Neubauer, C. Choi, R. Franckowski, S. Augustin, D.M. Iula, Tips for Interpreting GC MS Fragmentation of Unknown Substituted Fentanyls, Cayman Currents. 28 (2017) 1–3.
[87] C.A. Valdez, Gas Chromatography-Mass Spectrometry Analysis of Synthetic Opioids Belonging to the Fentanyl Class: A Review, Critical Reviews in Analytical Chemistry. 0 (2021) 1–31. https://doi.org/10.1080/10408347.2021.1927668.
[88] S.H. Hassanien, J.R. Bassman, C.M. Perrien Naccarato, J.J. Twarozynski, J.R. Traynor, D.M. Iula, J.P. Anand, In vitro pharmacology of fentanyl analogs at the human mu opioid receptor and their spectroscopic analysis, Drug Test Anal. 12 (2020) 1212–1221. https://doi.org/10.1002/dta.2822.
[89] A.D. Winokur, L.M. Kaufman, J.R. Almirall, Differentiation and identification of fentanyl analogues using GC-IRD, Forensic Chemistry. 20 (2020) 100255. https://doi.org/10.1016/j.forc.2020.100255.
[90] R.S. Vardanyan, V.J. Hruby, Fentanyl-related compounds and derivatives: current status and future prospects for pharmaceutical applications, Future Med Chem. 6 (2014) 385–412. https://doi.org/10.4155/fmc.13.215.
[91] P.O.M. Gundersen, A. Åstrand, H. Gréen, M. Josefsson, O. Spigset, S. Vikingsson, Metabolite Profiling of Ortho-, Meta- and Para-Fluorofentanyl by Hepatocytes and High-Resolution Mass Spectrometry, Journal of Analytical Toxicology. 44 (2020) 140–148. https://doi.org/10.1093/jat/bkz081.

[92] M.H. Baumann, G. Tocco, D.M. Papsun, A.L. Mohr, M.F. Fogarty, A.J. Krotulski, U-47700 and Its Analogs: Non-Fentanyl Synthetic Opioids Impacting the Recreational Drug Market, Brain Sciences. 10 (2020) 895. https://doi.org/10.3390/brainsci10110895.
[93] R. Solimini, S. Pichini, R. Pacifici, F.P. Busardò, R. Giorgetti, Pharmacotoxicology of Non-fentanyl Derived New Synthetic Opioids, Frontiers in Pharmacology. 9 (2018). https://www.frontiersin.org/article/10.3389/fphar.2018.00654 (accessed March 2, 2022).
[94] S.W. Fleming, J.C. Cooley, L. Johnson, C.C. Frazee, K. Domanski, K. Kleinschmidt, U. Garg, Analysis of U-47700, a Novel Synthetic Opioid, in Human Urine by LC–MS–MS and LC–QToF, J Anal Toxicol. (2016) jat;bkw131v1. https://doi.org/10.1093/jat/bkw131.
[95] M. Collins, D. Brown, S. Davies, B. Chan, B. Trotter, M. Moawad, K. Blakey, L. Collins-Brown, Case study: Identification and characterization of N-[2-(dimethylamino)cyclohexyl]-N-methylnaphthalene-2-carboxamide, a regioisomer of the synthetic opioid U10, Drug Testing and Analysis. 14 (2022) 188–195. https://doi.org/10.1002/dta.3133.
[96] E. Marchei, M.A. Ferri, M. Torrens, M. Farré, R. Pacifici, S. Pichini, M. Pellegrini, Ultra-High Performance Liquid Chromatography-High Resolution Mass Spectrometry and High-Sensitivity Gas Chromatography-Mass Spectrometry Screening of Classic Drugs and New Psychoactive Substances and Metabolites in Urine of Consumers, IJMS. 22 (2021) 4000. https://doi.org/10.3390/ijms22084000.
[97] D. Fabregat-Safont, X. Carbón, M. Ventura, I. Fornís, E. Guillamón, J.V. Sancho, F. Hernández, M. Ibáñez, Updating the list of known opioids through identification and characterization of the new opioid derivative 3,4-dichloro-N-(2-(diethylamino)cyclohexyl)-N-methylbenzamide (U-49900), Sci Rep. 7 (2017) 6338. https://doi.org/10.1038/s41598-017-06778-9.
[98] A.J. Krotulski, D.M. Papsun, S.E. Walton, B.K. Logan, Metonitazene in the United States—Forensic toxicology assessment of a potent new synthetic opioid using liquid chromatography mass spectrometry, Drug Testing and Analysis. 13 (2021) 1697–1711. https://doi.org/10.1002/dta.3115.
[99] M. Siczek, M. Zawadzki, M. Siczek, A. Chłopaś-Konowałek, P. Szpot, Etazene (N,N-diethyl-2-{[(4-ethoxyphenyl)methyl]-1H-benzimidazol-1-yl}-ethan-1-amine (dihydrochloride)): a novel benzimidazole opioid NPS identified in seized material: crystal structure and spectroscopic characterization, Forensic Toxicol. 39 (2021) 146–155. https://doi.org/10.1007/s11419-020-00552-9.
[100] I. Ujváry, R. Christie, M. Evans-Brown, A. Gallegos, R. Jorge, J. de Morais, R. Sedefov, DARK Classics in Chemical Neuroscience: Etonitazene and Related Benzimidazoles, ACS Chem. Neurosci. 12 (2021) 1072–1092. https://doi.org/10.1021/acschemneuro.1c00037.
[101] R.A. Jenkins, The fourth wave of the US opioid epidemic and its implications for the rural US: A federal perspective, Preventive Medicine. 152 (2021) 106541. https://doi.org/10.1016/j.ypmed.2021.106541.
[102] J. Lamsma, W. Cahn, S. Fazel, GROUP and NEDEN investigators, Use of illicit substances and violent behaviour in psychotic disorders: two nationwide case-control studies and meta-analyses, Psychol. Med. 50 (2020) 2028–2033. https://doi.org/10.1017/S0033291719002125.
[103] M.P. Levitas, E. Andrews, I. Lurie, I. Marginean, Discrimination of synthetic cathinones by GC–MS and GC–MS/MS using cold electron ionization, Forensic Science International. 288 (2018) 107–114. https://doi.org/10.1016/j.forsciint.2018.04.026.

[104] M.L. Banks, T.J. Worst, D.E. Rusyniak, J.E. Sprague, Synthetic Cathinones ("Bath Salts"), The Journal of Emergency Medicine. 46 (2014) 632–642. https://doi.org/10.1016/j.jemermed.2013.11.104.
[105] E. Pieprzyca, R. Skowronek, Ľ. Nižnanský, P. Czekaj, Synthetic cathinones – From natural plant stimulant to new drug of abuse, European Journal of Pharmacology. 875 (2020) 173012. https://doi.org/10.1016/j.ejphar.2020.173012.
[106] J. Bonetti, Mass spectral differentiation of positional isomers using multivariate statistics, Forensic Chemistry. 9 (2018) 50–61. https://doi.org/10.1016/j.forc.2018.06.001.
[107] S. Kerrigan, M. Savage, C. Cavazos, P. Bella, Thermal Degradation of Synthetic Cathinones: Implications for Forensic Toxicology, Journal of Analytical Toxicology. 40 (2016) 1–11. https://doi.org/10.1093/jat/bkv099.
[108] D. Zuba, Identification of cathinones and other active components of 'legal highs' by mass spectrometric methods, TrAC Trends in Analytical Chemistry. 32 (2012) 15–30. https://doi.org/10.1016/j.trac.2011.09.009.
[109] M.K. Woźniak, M. Wiergowski, J. Aszyk, P. Kubica, J. Namieśnik, M. Biziuk, Application of gas chromatography–tandem mass spectrometry for the determination of amphetamine-type stimulants in blood and urine, Journal of Pharmaceutical and Biomedical Analysis. 148 (2018) 58–64. https://doi.org/10.1016/j.jpba.2017.09.020.
[110] M. Ferrucci, F. Limanaqi, L. Ryskalin, F. Biagioni, C.L. Busceti, F. Fornai, The Effects of Amphetamine and Methamphetamine on the Release of Norepinephrine, Dopamine and Acetylcholine From the Brainstem Reticular Formation, Frontiers in Neuroanatomy. 13 (2019). https://www.frontiersin.org/article/10.3389/fnana.2019.00048 (accessed March 7, 2022).
[111] S.B. Sachs, F. Woo, A Detailed Mechanistic Fragmentation Analysis of Methamphetamine and Select Regioisomers by GC/MS, J Forensic Sci. 52 (2007) 308–319. https://doi.org/10.1111/j.1556-4029.2007.00401.x.
[112] M.A. Bodnar Willard, V.L. McGuffin, R.W. Smith, Statistical comparison of mass spectra for identification of amphetamine-type stimulants, Forensic Science International. 270 (2017) 111–120. https://doi.org/10.1016/j.forsciint.2016.11.013.
[113] G. Mercieca, S. Odoardi, M. Cassar, S. Strano Rossi, Rapid and simple procedure for the determination of cathinones, amphetamine-like stimulants and other new psychoactive substances in blood and urine by GC–MS, Journal of Pharmaceutical and Biomedical Analysis. 149 (2018) 494–501. https://doi.org/10.1016/j.jpba.2017.11.024.
[114] V. Cocchi, S. Gasperini, P. Hrelia, M. Tirri, M. Marti, M. Lenzi, Novel Psychoactive Phenethylamines: Impact on Genetic Material, International Journal of Molecular Sciences. 21 (2020) 9616. https://doi.org/10.3390/ijms21249616.
[115] A.L. Setser, R. Waddell Smith, Comparison of variable selection methods prior to linear discriminant analysis classification of synthetic phenethylamines and tryptamines, Forensic Chemistry. 11 (2018) 77–86. https://doi.org/10.1016/j.forc.2018.10.002.
[116] P. Adamowicz, B. Tokarczyk, Simple and rapid screening procedure for 143 new psychoactive substances by liquid chromatography-tandem mass spectrometry: Simple and rapid screening procedure for 143 new psychoactive substances, Drug Test. Analysis. 8 (2016) 652–667. https://doi.org/10.1002/dta.1815.
[117] B.-H. Chen, J.-T. Liu, H.-M. Chen, W.-X. Chen, C.-H. Lin, Comparison of the Characteristic Mass Fragmentations of Phenethylamines and Tryptamines by Electron Ionization Gas Chromatography Mass Spectrometry, Electrospray and Matrix-Assisted Laser

Desorption Ionization Mass Spectrometry, Applied Sciences. 8 (2018) 1022. https://doi.org/10.3390/app8071022.
[118] S.R. Rose, J.L. Poklis, A. Poklis, A case of 25I-NBOMe (25-I) intoxication: a new potent 5-HT2A agonist designer drug, Clin Toxicol (Phila). 51 (2013) 174–177. https://doi.org/10.3109/15563650.2013.772191.
[119] B.V. Dean, S.J. Stellpflug, A.M. Burnett, K.M. Engebretsen, 2C or Not 2C: Phenethylamine Designer Drug Review, J Med Toxicol. 9 (2013) 172–178. https://doi.org/10.1007/s13181-013-0295-x.
[120] M. Hansen, K. Phonekeo, J.S. Paine, S. Leth-Petersen, M. Begtrup, H. Bräuner-Osborne, J.L. Kristensen, Synthesis and Structure–Activity Relationships of N-Benzyl Phenethylamines as 5-HT2A/2C Agonists, ACS Chem. Neurosci. 5 (2014) 243–249. https://doi.org/10.1021/cn400216u.
[121] A.L. Halberstadt, M. Chatha, A. Stratford, M. Grill, S.D. Brandt, Comparison of the behavioral responses induced by phenylalkylamine hallucinogens and their tetrahydrobenzodifuran ("FLY") and benzodifuran ("DragonFLY") analogs, Neuropharmacology. 144 (2019) 368–376. https://doi.org/10.1016/j.neuropharm.2018.10.037.
[122] D.E. Nichols, W.E. Fantegrossi, Chapter Nineteen - Emerging Designer Drugs, in: B. Madras, M. Kuhar (Eds.), The Effects of Drug Abuse on the Human Nervous System, Academic Press, Boston, 2014: pp. 575–596. https://doi.org/10.1016/B978-0-12-418679-8.00019-8.
[123] K. Kanai, K. Takekawa, T. Kumamoto, T. Ishikawa, T. Ohmori, Simultaneous analysis of six phenethylamine-type designer drugs by TLC, LC-MS, and GC-MS, Forensic Toxicol. 26 (2008) 6–12. https://doi.org/10.1007/s11419-008-0041-2.
[124] B. Anilanmert, F. Çavuş, I. Narin, S. Cengiz, Ş. Sertler, A.A. Özdemir, M. Açikkol, Simultaneous analysis method for GHB, ketamine, norketamine, phenobarbital, thiopental, zolpidem, zopiclone and phenytoin in urine, using C18 poroshell column, Journal of Chromatography B. 1022 (2016) 230–241. https://doi.org/10.1016/j.jchromb.2016.03.040.
[125] M.D. Arbo, M.L. Bastos, H.F. Carmo, Piperazine compounds as drugs of abuse, Drug and Alcohol Dependence. 122 (2012) 174–185. https://doi.org/10.1016/j.drugalcdep.2011.10.007.
[126] R.-H. Zhang, H.-Y. Guo, H. Deng, J. Li, Z.-S. Quan, Piperazine skeleton in the structural modification of natural products: a review, Journal of Enzyme Inhibition and Medicinal Chemistry. 36 (2021) 1165–1197. https://doi.org/10.1080/14756366.2021.1931861.
[127] M.A. Al-Omar, Synthesis and Antimicrobial Activity of New 5-(2-Thienyl)-1,2,4-triazoles and 5-(2-Thienyl)-1,3,4-oxadiazoles and Related Derivatives, Molecules. 15 (2010) 502–514. https://doi.org/10.3390/molecules15010502.
[128] D. Zuba, K. Sekuła, Identification and characterization of 2,5-dimethoxy-3,4-dimethyl-β-phenethylamine (2C-G)--a new designer drug, Drug Test Anal. 5 (2013) 549–559. https://doi.org/10.1002/dta.1396.
[129] D. Zuba, K. Sekuła, A. Buczek, Identification and characterization of 2,5-dimethoxy-4-nitro-β-phenethylamine (2C-N) – A new member of 2C-series of designer drug, Forensic Science International. 222 (2012) 298–305. https://doi.org/10.1016/j.forsciint.2012.07.006.
[130] B. Sanders, S.E. Lankenau, J.J. Bloom, D. Hathazi, "Research Chemicals": Tryptamine and Phenethylamine Use Among High-Risk Youth, Subst Use Misuse. 43 (2008) 389–402. https://doi.org/10.1080/00952990701202970.

[131] A.D. Volgin, O.A. Yakovlev, K.A. Demin, P.A. Alekseeva, E.J. Kyzar, C. Collins, D.E. Nichols, A.V. Kalueff, Understanding Central Nervous System Effects of Deliriant Hallucinogenic Drugs through Experimental Animal Models, ACS Chem. Neurosci. 10 (2019) 143–154. https://doi.org/10.1021/acschemneuro.8b00433.
[132] M. Kokkinou, A.H. Ashok, O.D. Howes, The effects of ketamine on dopaminergic function: meta-analysis and review of the implications for neuropsychiatric disorders, Mol Psychiatry. 23 (2018) 59–69. https://doi.org/10.1038/mp.2017.190.
[133] A. Mozayani, Phencyclidine - Effects on Human Performance and Behavior, Forensic Sci Rev. 15 (2003) 61–74.
[134] F. Zamberlan, C. Sanz, R. Martínez Vivot, C. Pallavicini, F. Erowid, E. Erowid, E. Tagliazucchi, The Varieties of the Psychedelic Experience: A Preliminary Study of the Association Between the Reported Subjective Effects and the Binding Affinity Profiles of Substituted Phenethylamines and Tryptamines, Frontiers in Integrative Neuroscience. 12 (2018). https://www.frontiersin.org/article/10.3389/fnint.2018.00054 (accessed March 16, 2022).
[135] S. Malaca, A.F. Lo Faro, A. Tamborra, S. Pichini, F.P. Busardò, M.A. Huestis, Toxicology and Analysis of Psychoactive Tryptamines, IJMS. 21 (2020) 9279. https://doi.org/10.3390/ijms21239279.
[136] J. Castelhano, G. Lima, M. Teixeira, C. Soares, M. Pais, M. Castelo-Branco, The Effects of Tryptamine Psychedelics in the Brain: A meta-Analysis of Functional and Review of Molecular Imaging Studies, Frontiers in Pharmacology. 12 (2021). https://www.frontiersin.org/article/10.3389/fphar.2021.739053 (accessed March 15, 2022).
[137] A.M. Araújo, F. Carvalho, M. de L. Bastos, P. Guedes de Pinho, M. Carvalho, The hallucinogenic world of tryptamines: an updated review, Arch Toxicol. 89 (2015) 1151–1173. https://doi.org/10.1007/s00204-015-1513-x.
[138] C. Wallwey, S.-M. Li, Ergot alkaloids : structure diversity, biosynthetic gene clusters and functional proof of biosynthetic genes, Natural Product Reports. 28 (2011) 496–510. https://doi.org/10.1039/C0NP00060D.
[139] R. Tittarelli, G. Mannocchi, F. Pantano, F.S. Romolo, Recreational Use, Analysis and Toxicity of Tryptamines, Curr Neuropharmacol. 13 (2015) 26–46. https://doi.org/10.2174/1570159X13666141210222409.
[140] S.D. Brandt, C.P.B. Martins, Analytical methods for psychoactive N,N-dialkylated tryptamines, TrAC Trends in Analytical Chemistry. 29 (2010) 858–869. https://doi.org/10.1016/j.trac.2010.04.008.
[141] S.L. Greene, Chapter 15 - Tryptamines, in: P.I. Dargan, D.M. Wood (Eds.), Novel Psychoactive Substances, Academic Press, Boston, 2013: pp. 363–381. https://doi.org/10.1016/B978-0-12-415816-0.00015-8.
[142] B.-H. Chen, J.-T. Liu, W.-X. Chen, H.-M. Chen, C.-H. Lin, A general approach to the screening and confirmation of tryptamines and phenethylamines by mass spectral fragmentation, Talanta. 74 (2008) 512–517. https://doi.org/10.1016/j.talanta.2007.06.012.
[143] A. Gaujac, S.T. Martinez, A.A. Gomes, S.J. de Andrade, A. da C. Pinto, J.M. David, S. Navickiene, J.B. de Andrade, Application of analytical methods for the structural characterization and purity assessment of N,N-dimethyltryptamine, a potent psychedelic agent isolated from Mimosa tenuiflora inner barks, Microchemical Journal. 109 (2013) 78–83. https://doi.org/10.1016/j.microc.2012.03.033.

[144] S. Brandt, P. Kavanagh, F. Westphal, A. Stratford, S. Elliott, K. Hoang, J. Wallach, A. Halberstadt, Return of the lysergamides. Part I: Analytical and behavioural characterization of 1-propionyl-d-lysergic acid diethylamide (1P-LSD)., Drug Testing and Analysis. (2016). https://doi.org/10.1002/dta.1884.

[145] C.C. Nelson, R.L. Foltz, Determination of lysergic acid diethylamide (LSD), iso-LSD, and N-demethyl-LSD in body fluids by gas chromatography/tandem mass spectrometry, Anal. Chem. 64 (1992) 1578–1585. https://doi.org/10.1021/ac00038a014.

[146] E. Sisco, T.P. Forbes, Forensic applications of DART-MS: A review of recent literature, Forensic Chemistry. 22 (2021) 100294. https://doi.org/10.1016/j.forc.2020.100294.

[147] P. Kriikku, A. Pelander, I. Rasanen, I. Ojanperä, Toxic lifespan of the synthetic opioid U-47,700 in Finland verified by re-analysis of UPLC-TOF-MS data, Forensic Science International. 300 (2019) 85–88. https://doi.org/10.1016/j.forsciint.2019.04.030.

[148] S. Salle, S. Bodeau, A. Dhersin, M. Ferdonnet, R. Goncalves, M. Lenski, B. Lima, M. Martin, J. Outreville, J. Vaucel, N. Fabresse, Novel synthetic opioids: A review of the literature, Toxicologie Analytique et Clinique. 31 (2019) 298–316. https://doi.org/10.1016/j.toxac.2019.10.001.

[149] B.P. Mayer, A.J. DeHope, D.A. Mew, P.E. Spackman, A.M. Williams, Chemical Attribution of Fentanyl Using Multivariate Statistical Analysis of Orthogonal Mass Spectral Data, Anal. Chem. 88 (2016) 4303–4310. https://doi.org/10.1021/acs.analchem.5b04434.

[150] S. Qiao, H. Xu, W. Zhang, W. Yang, D. Guo, W. Wang, W. Xu, Y. Liu, G. Liu, Y. Cui, H. Yu, Q. Li, Identification of characteristic heroin metabolites in urine based on data-mining technology and multivariate statistics analysis combined with a targeted verification approach for distinguishing heroin abusers, Journal of Chromatography B. 1152 (2020) 122251. https://doi.org/10.1016/j.jchromb.2020.122251.

Supplemental Information

Figure S1: InChIKey definition and comparison between the SWGDRUG and Cayman Chemical databases for heroin.

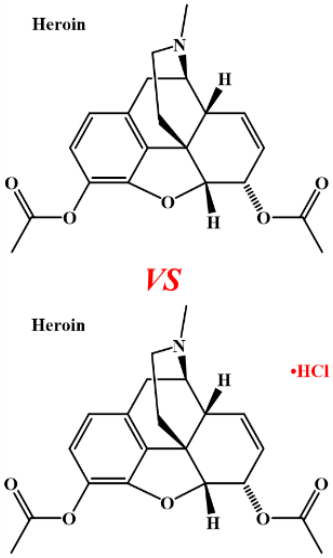

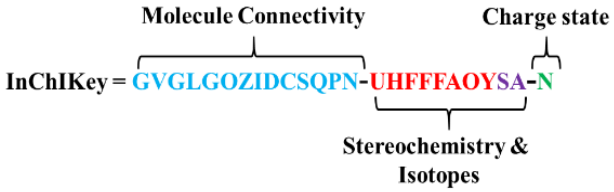

Database (form)	InChIKey entry
SWGDRUG (base)	GVGLGOZIDCSQPN-UHFFFAOYSA-N
Cayman Chemical (base)	GVGLGOZIDCSQPN-PVHGPHFFSA-N
Cayman Chemical (HCl salt)	FZJYQGFGNHGSFX-PVQKIFDLSA-N

Merging Cayman Chemical Class with SWGDRUG Spectra

To associate the Cayman Chemical classes with the SWGDRUG entries, several preprocessing steps were first required to merge this information. Using the statistical program *R* (*R*Studio, Inc., Austria) as a platform, certain entries were omitted to obtain uniformity for an optimal merge. For the SWGDRUG database, entries containing the deuterated forms of compounds and metabolites were excluded. The Cayman Chemical product list possesses salt adducts of illicit substances which is troublesome when matching by a substance name because that information is included along with a compound's identifier. Therefore, the lingering salt adducts (*i.e.*, ·HCl) along with the associated names were stripped from the substance entry. Once removed, new InChIKeys, which are unique entries consisting of three blocks of information, were generated for the new free-base form of the Cayman Chemical compounds using OpenBabel software.

The information from the SWGDRUG and Cayman Chemical product list were merged via the 14-block connectivity segment of the InChIKeys. This portion was chosen because the connectivity of the substance remains constant whereas stereochemistry may not be recorded. After the merge, duplicate entries were removed, and the newly formed database was checked for consistencies and accuracy. The results of this process yielded over 1,500 entries with six broad class and fourteen subclass assignments (**Table 1**) along with the SWGDRUG mass spectral data.

Requirements for data analysis. The program was designed to evaluate EI-MS data and collate a database. This program was written using *R 4.2.10*[1]. External R-packages used in the program include *data.table*[2], *readxl*[3]. Specific application of functions from each external package will be described as required. In addition, Open Babel[4,5] functionality was used to convert between chemical structure formats.

Step 1. Import information. Data were converted to an .RDS format prior to preprocessing.

Step 2. Homogenize information. Unnecessary column information was omitted from both Cayman Chemical and SWGDRUG lists including "comments", "item number", and "CAS number". Entries containing the deuterated forms of substances, method information, and specific purposes (*i.e.*, Cannabinoid Research and Angiogenesis) were omitted. Salt information both in the compound name and the chemical formula were stripped from the entries. Duplicates were also removed from each dataset.

Step 3. InChIKey generation and merge. Structure conversions are done via Open Babel to generate new InChIKeys from the stripped salt entries. The open babel commands are run per compound in the files and converts from SMILES to InChIKey. Because stereochemistry alters the InChIKey entries, the connectivity portion was used to merge the Cayman Chemical and SWGDRUG datasets. Once merged, duplicates were removed, and the remaining database was checked for accuracy.

Software Availability

Base R (https://www.r-project.org/) and Open Babel (https://openbabel.org/wiki/Main_Page) are freely available and the version appropriate for the users operating system should be installed prior to running and analyzing the merged database.

---

[1]R Core Team (2019). R: A language and environment for statistical computing. R Foundation for Statistical Computing, Vienna, Austria. URL https://www.R-project.org/.

[2]Matt Dowle and Arun Srinivasan (2019). data.table: Extension of `data.frame`. R package version 1.12.8. https://CRAN.R-project.org/package=data.table

[3]Hadley Wickham and Jennifer Bryan (2019). readxl: Read Excel Files. R package version 1.3.1. https://CRAN.R-project.org/package=readxl

[4]http://openbabel.org/wiki/Main_Page

[5]O'Boyle, N. M., Banck, M., James, C. A., Morley, C., Vandermeersch, T., & Hutchison, G. R. (2011). Open Babel: An open chemical toolbox. *Journal of cheminformatics*, 3(1), 33

Practice Examples

This section compiles the ion distribution information presented in the manuscript for quick reference. For clarity, the leftmost figure depicts the average distribution of *Low* (light blue), *Medium* (blue), and *High + Base Peak* (dark blue) across the *m/z* range. The center figure represents the average number of peaks for each RA category (excluding *Ultra-Low*) and the y-axis is locked to allow for easier comparisons. The rightmost figure highlights the frequency and presence and RA of molecular ions. Following these figures are three "unknown" mass spectra along with brief descriptions on how the data present in this manuscript can be used to classify the unknown substance.

Barbiturates

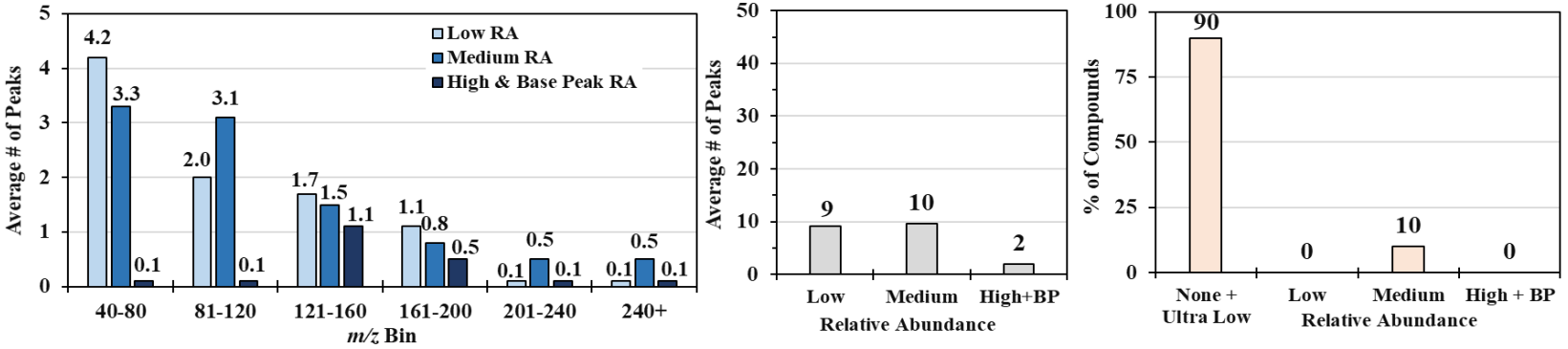

Benzodiazepines

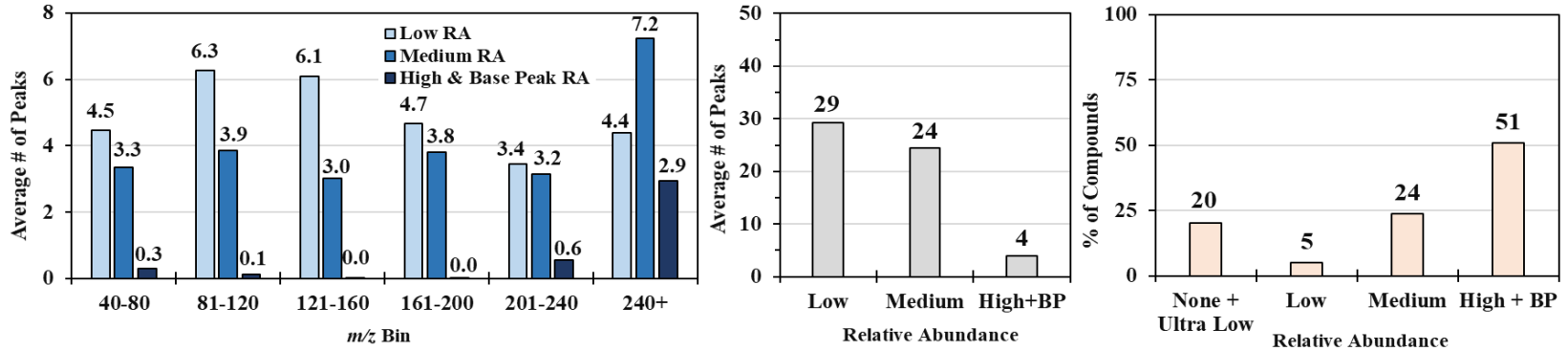

Anabolic Steroids

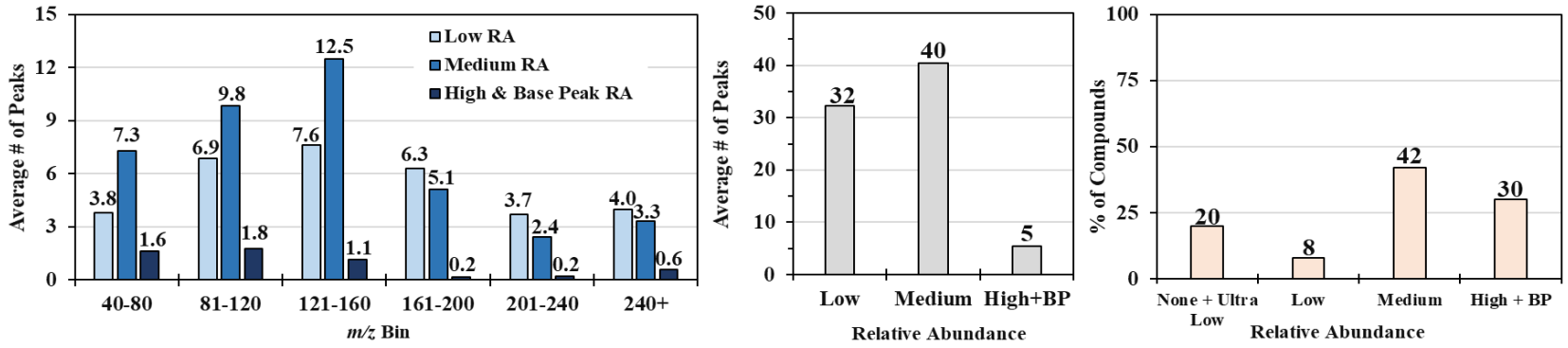

Phytocannabinoids

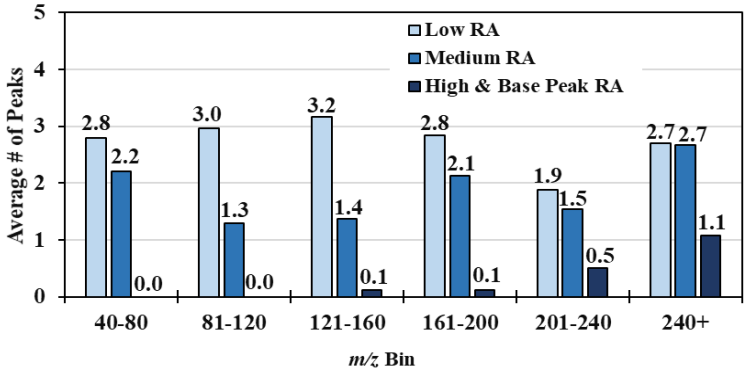

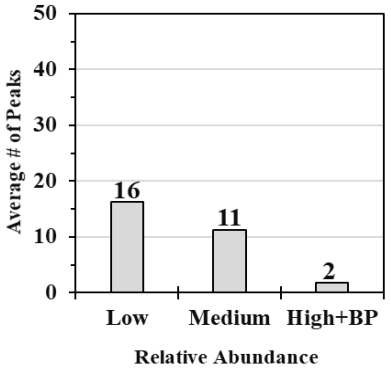

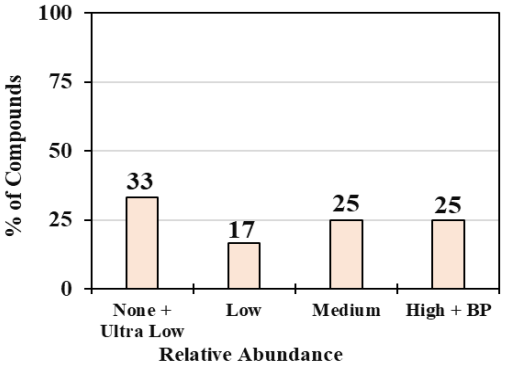

Synthetic Cannabinoids

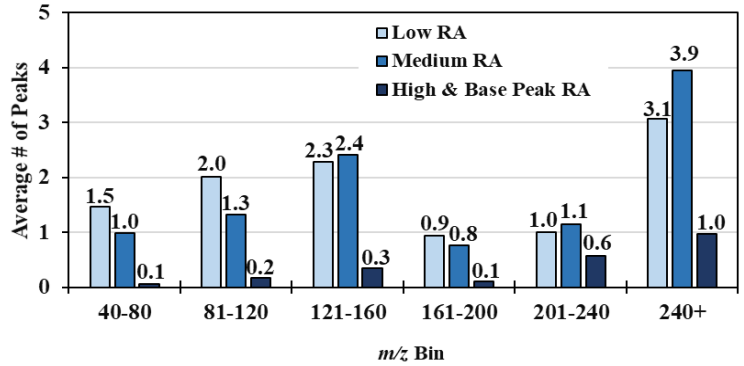

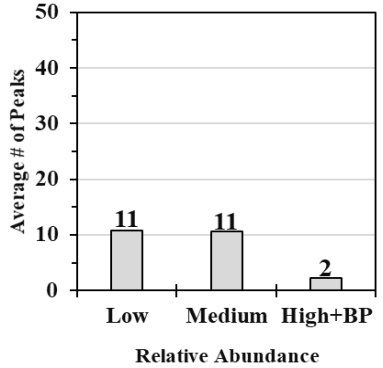

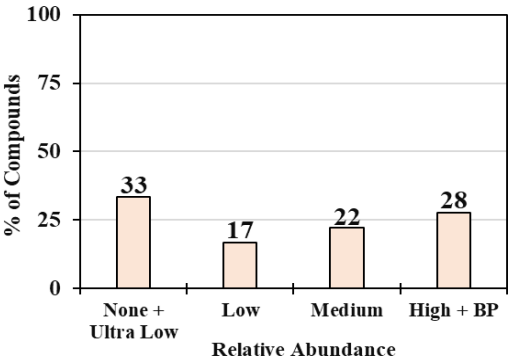

Opiates

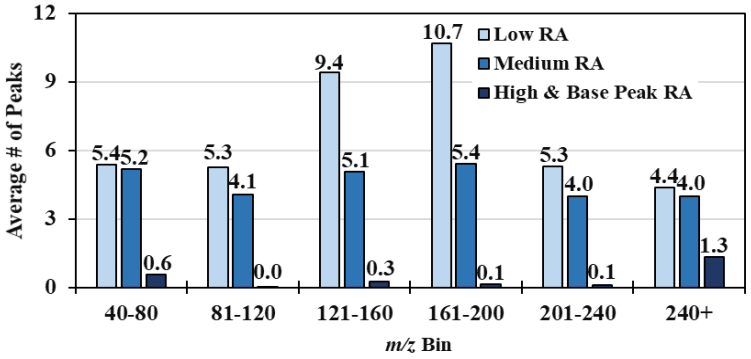

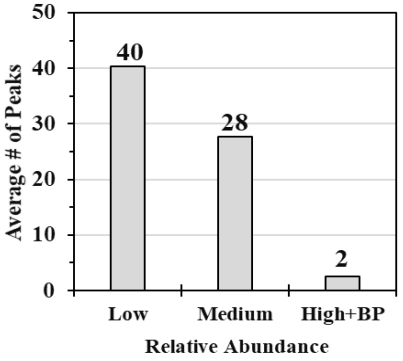

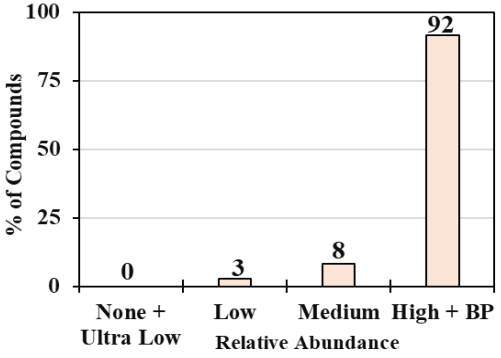

Fentanyls

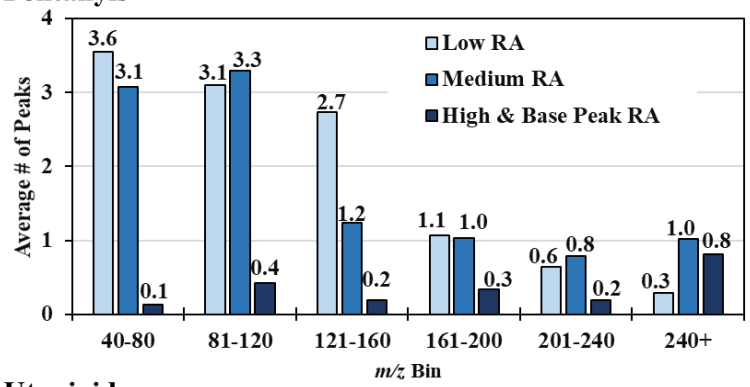

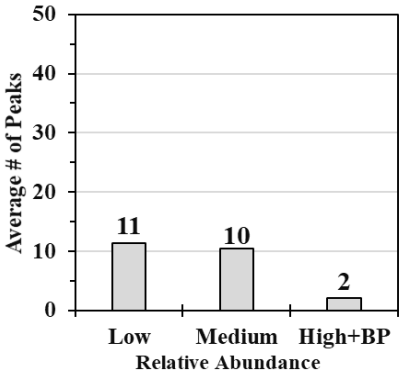

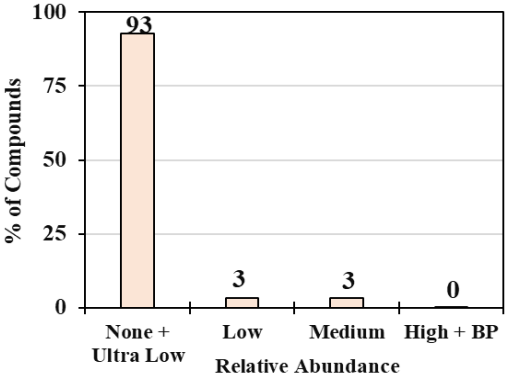

Utopioids

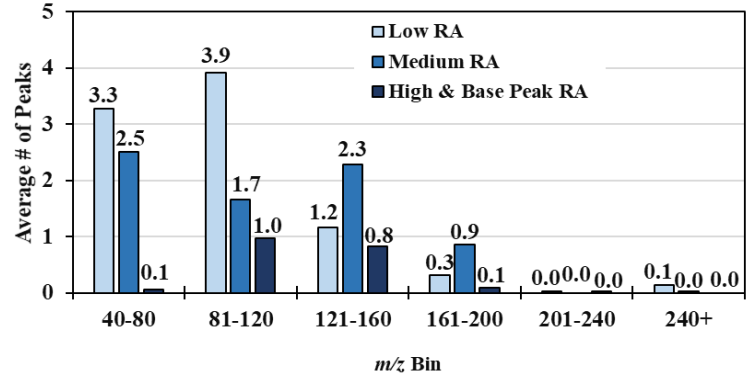

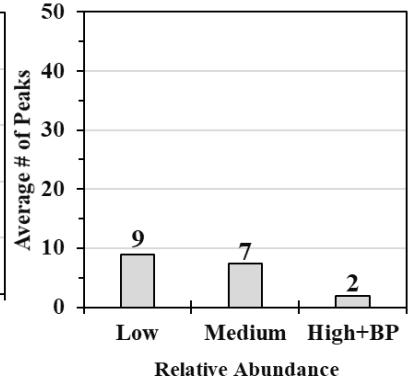

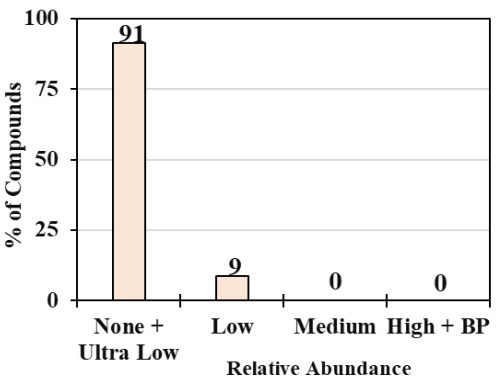

Nitazenes

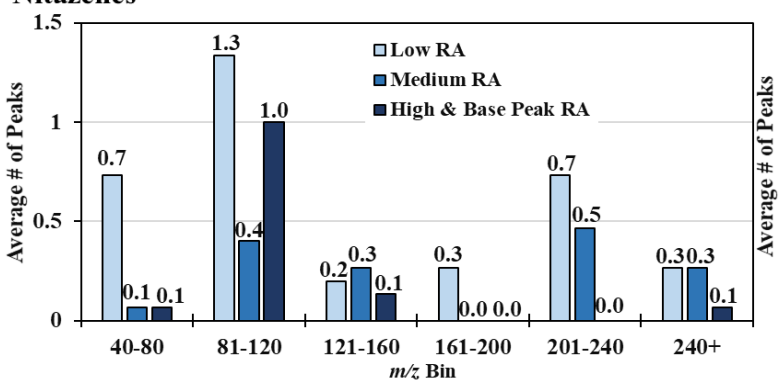

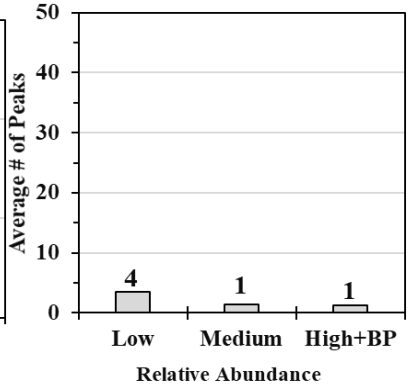

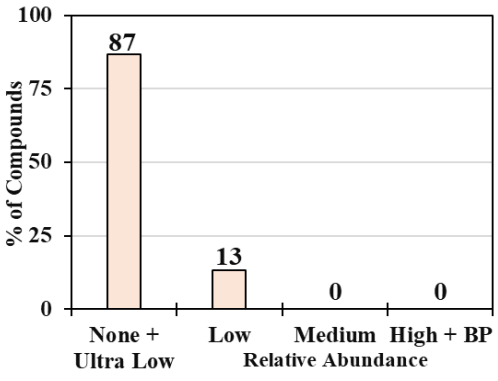

Cathinones

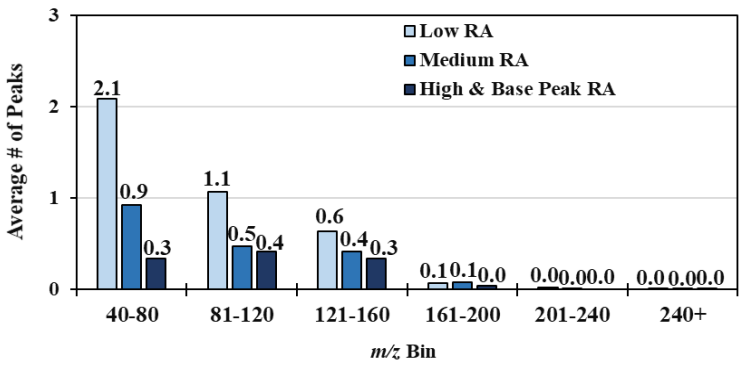

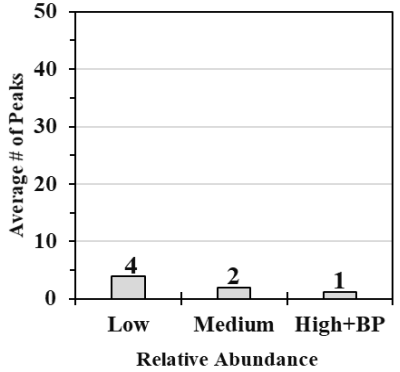

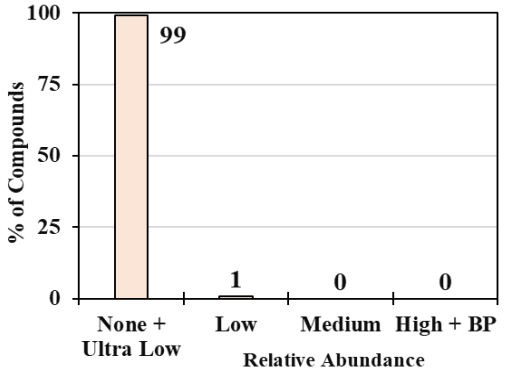

Amphetamines

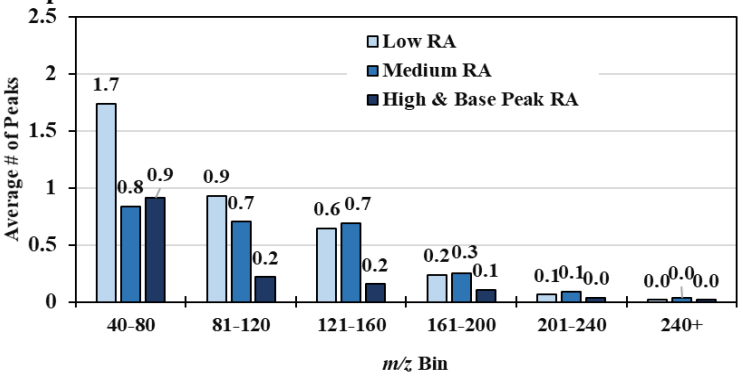

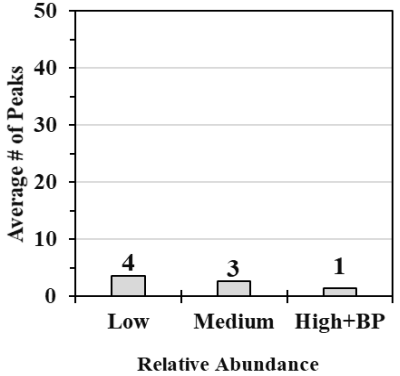

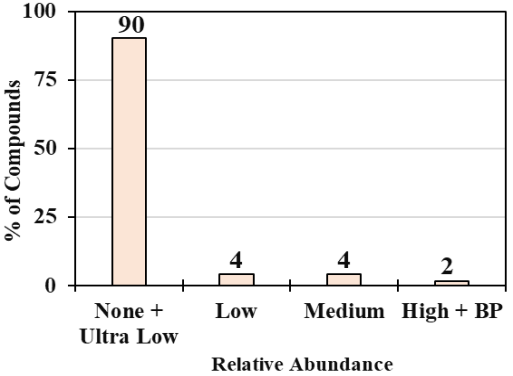

Phenethylamines

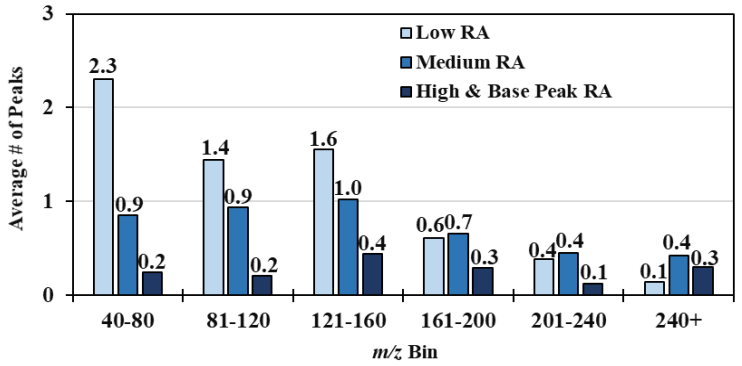

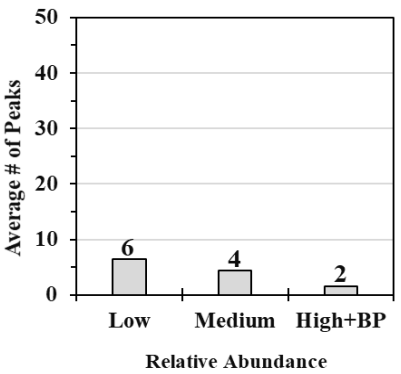

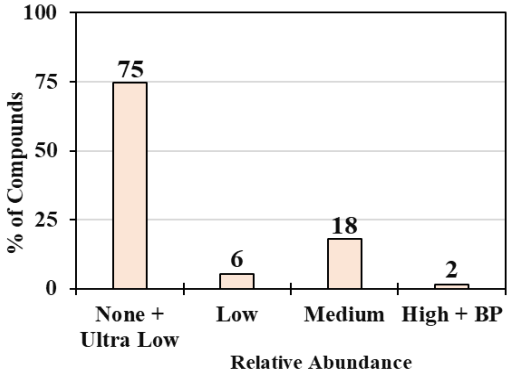

Arylcyclohexylamines

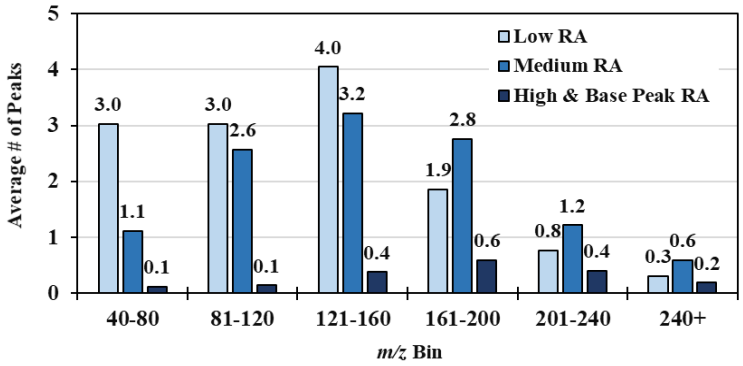

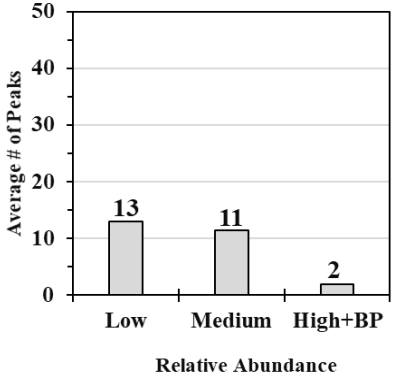

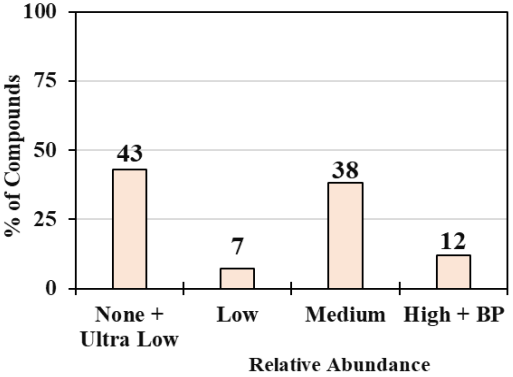

Piperazines

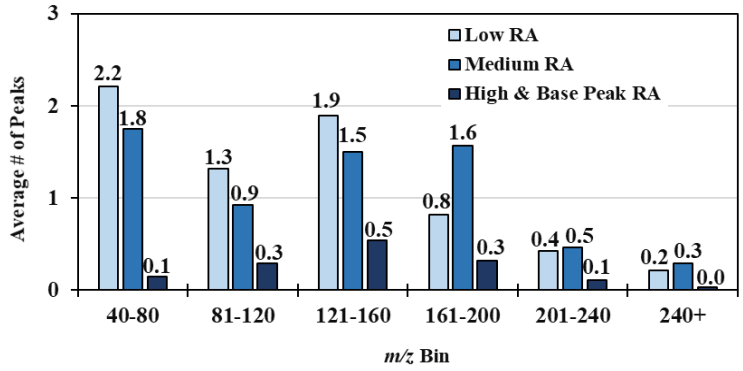

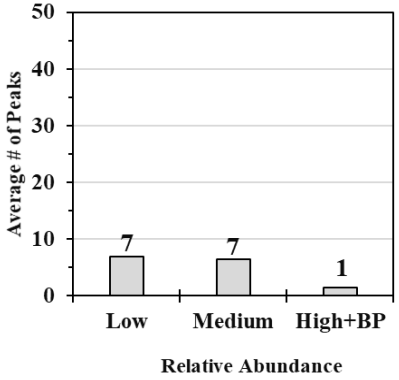

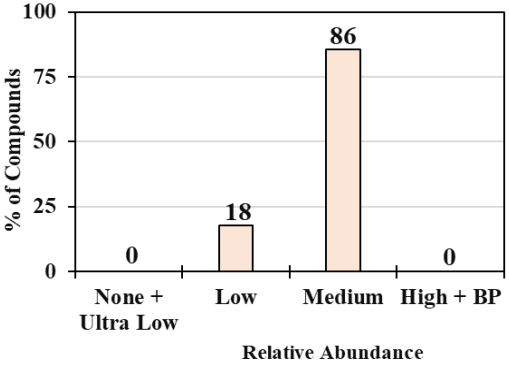

Tryptamines

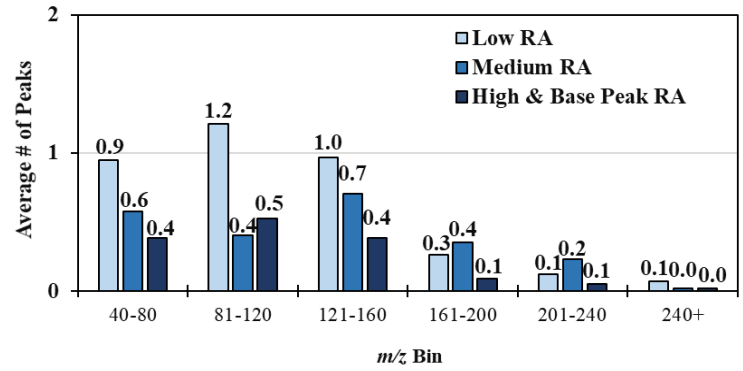

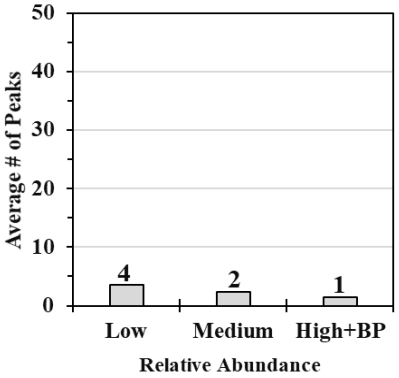

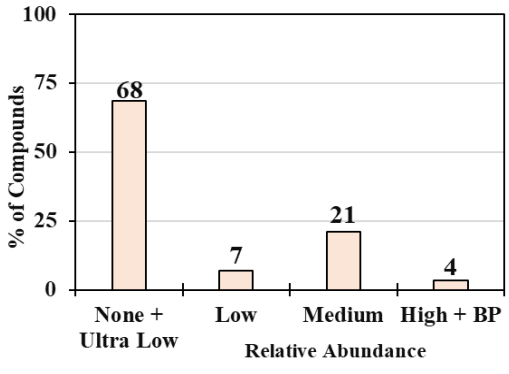

Example 1 – Butonitazene

- *Observation:* A feature-poor mass spectrum with no notable *m/z* values above 300.
  - Classes ruled out – barbituates, benzodiazepines, anabolic steroids, cannabinoids (phyto- and synthetic), opiates, fentanyls, utopioids, arylcyclohexylamines, and piperaizines based on this observation.
- *Observaion:* A molecular ion is not present with an appreciable RA.
  - Cannot rule out any additional classes.
- *Observation:* There is a *Base Peak* at *m/z* 86 with no other *High* RA peaks.
  - Based on the peak tables, all remaining classes except nitazenes, cathinones, or tryptamines are ruled out.
- *Observation:* There are two other notable peaks at *m/z* 58 and *m/z* 107.

The presence of *m/z* 86, *m/z* 58, and *m/z* 107 indicates, based on the peak tables, that this compound is likely a nitazene.

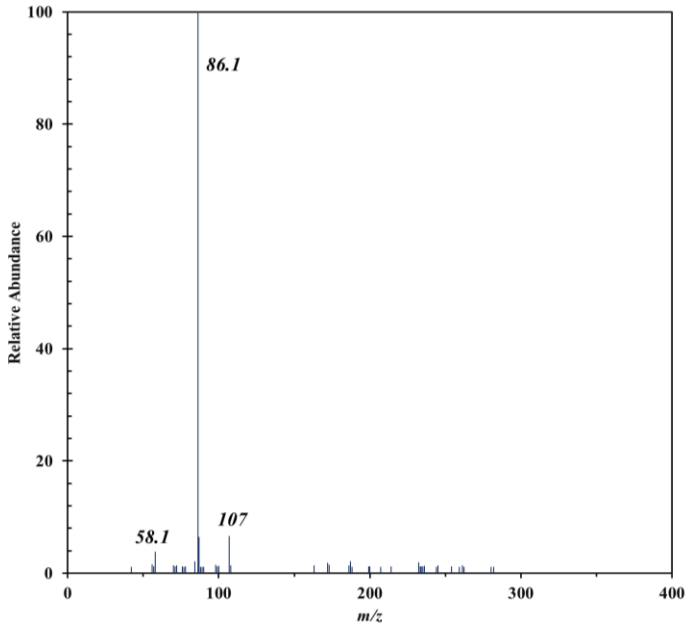

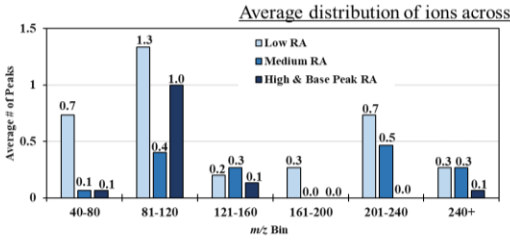

Average distribution of ions across *m/z* range

High + BP	*Medium*	*Low*
240+ = 0	240+ = 0	240+ = 0
201-240 = 0	201-240 = 0	201-240 = 0
161-200 = 0	161-200 = 0	161-200 = 0
121-160 = 0	121-160 = 0	121-160 = 0
81-120 = 1	81-120 = 0	81-120 = 1
40-80 = 0	40-80 = 0	40-80 = 1

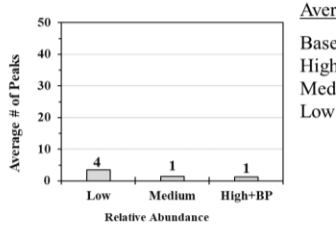

Average peaks per RA

Base Peak = 1
High = 0
Medium = 1
Low = 3

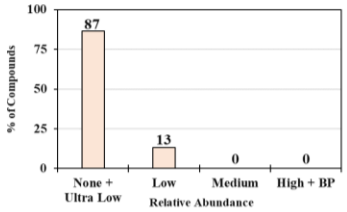

Frequency presence of $M^{+\bullet}$ per RA

Molecular Ion = *Ultra-Low*

Example 2 – Fluorexetamine

- *Observation:* Mass spectrum has no notable *m/z* values above 300 Da but there are many ion of*Medium* RA across the less than *m/z* 200 range.
    - Compound could be a fentanyl, arylcyclohexylamine, and piperazine.
- *Observation:* There is a *Base Peak* at *m/z* 178 and what seems to be an *Ultra-Low* molecular ion at *m/z* 235.
    - Based on the peak tables, we can rule out this compound being a fentanyl.
- *Observation:* Assuming a molecular ion of *m/z* 235, the major neutral losses from are 28 Da, 57 Da, and 85 Da, respectively.

These neutral losses may indicate more of the arylcyclohexylamine class with a ketone substitution.

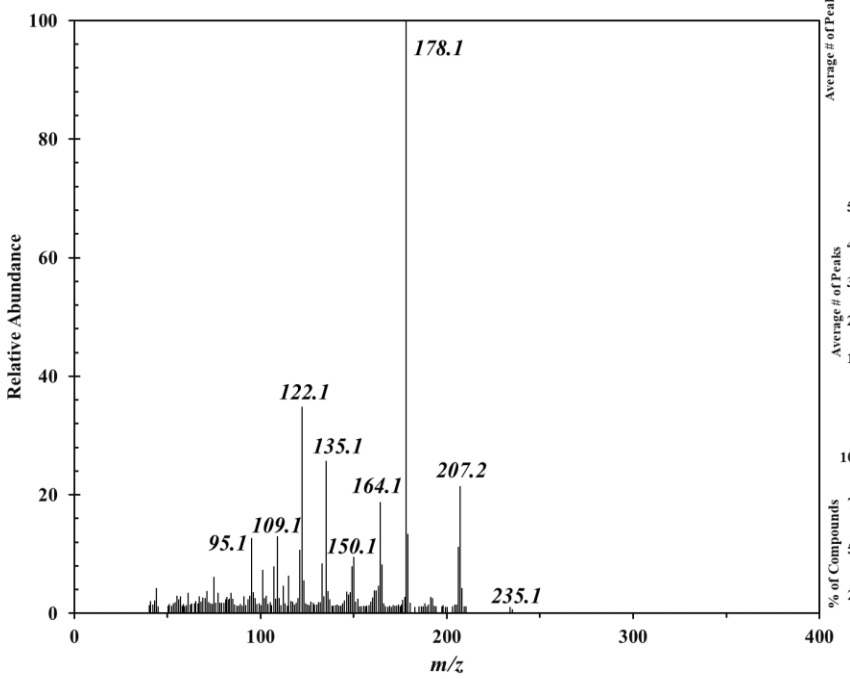

Average distribution of ions across *m/z* range

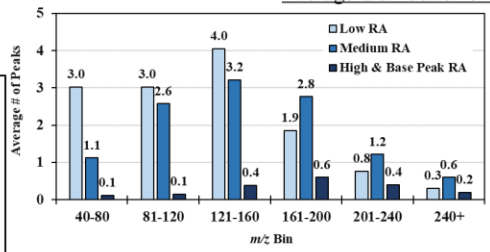

High + BP	*Medium*	*Low*
240+ = 0	240+ = 0	240+ = 0
201-240 = 0	201-240 = 1	201-240 = 1
161-200 = 1	161-200 = 1	161-200 = 2
121-160 = 0	121-160 = 4	121-160 = 3
81-120 = 0	81-120 = 2	81-120 = 4
40-80 = 0	40-80 = 0	40-80 = 3

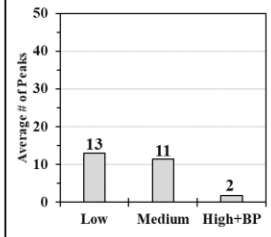

Average peaks per RA

Base Peak = 1
High = 0
Medium = 6
Low = 4

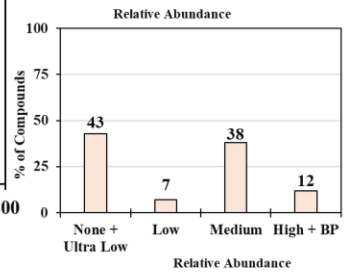

Frequency presence of $M^{+\bullet}$ per RA

Molecular Ion = *Ultra-Low*

Example 3 – AB-CHMINACA

- *Observation:* The mass spectrum a has several major peaks near and above *m/z* 240.
  - Compound is likely in either the benzodiazepine, phytocannabinoid, or synthetic cannabinoid class.
- *Observation:* A molecular ion is present, but at a *Low* RA.
  - Compound is likely not a benzodiazepine and is likely either a phytocannabinoid or synthetic cannabinoid.
- *Observation:* There is a *Base Peak* at *m/z* 241 with *Medium* RA peaks at *m/z* 145 and *m/z* 312. Assuming a molecular ion of *m/z* 356 indicates major neutral losses of 44 Da, 115 Da, and 211 Da.

Based on the peak tables, and neutral loss tables, this compound is likely a synthetic cannabinoid, not a phytocanabinoid.

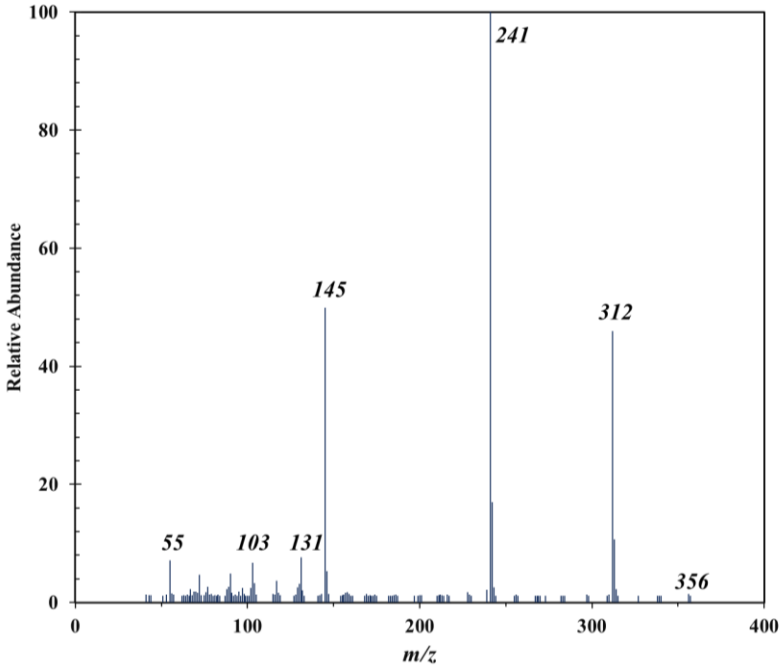

Average distribution of ions across *m/z* range

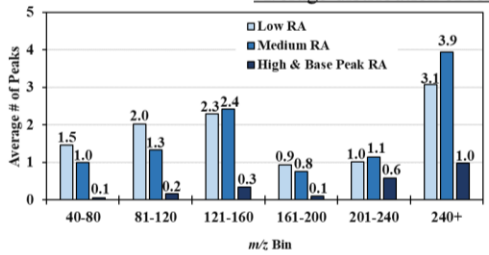

High + BP	*Medium*	*Low*
240+ = 1	240+ = 1	240+ = 0
201-240 = 0	201-240 = 0	201-240 = 0
161-200 = 1	161-200 = 0	161-200 = 0
121-160 = 0	121-160 = 1	121-160 = 1
81-120 = 0	81-120 = 0	81-120 = 1
40-80 = 0	40-80 = 0	40-80 = 3

Average peaks per RA

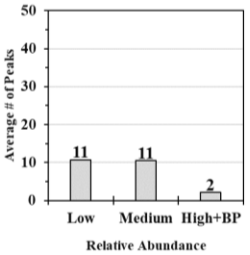

Base Peak = 1
High =0
Medium = 3
Low = 10

Frequency presence of $M^{+\bullet}$ per RA

Molecular Ion = *Ultra-Low*